Modeling and analysis of Duhem hysteresis operators with butterfly loops

Vasquez Beltran, Marco; Jayawardhana, Bayu; Peletier, Reynier

Published in:
ArXiv

Publication date:
2021

Modeling and analysis of Duhem hysteresis operators with butterfly loops

M. A. Vasquez-Beltran, B. Jayawardhana, R. F. Peletier

***Abstract*—In this work we study and analyze a class of Duhem hysteresis operators that can exhibit butterfly loops. We study firstly the consistency property of such operator which corresponds to the existence of an attractive periodic solution when the operator is subject to a periodic input signal. Subsequently, we study the two defining functions of the Duhem operator such that the corresponding periodic solutions can admit a butterfly input-output phase plot. We present a number of examples where the Duhem butterfly hysteresis operators are constructed using two zero-level set curves that satisfy some mild conditions.**

I. INTRODUCTION

Hysteresis is a natural phenomenon that was originally investigated in the study of magnetic field and magnetic flux density in ferromagnetic materials [1]. In the following centuries, the hysteresis phenomena are well-documented and studied in numerous systems originating from various disciplines, from biology [2], [3], physics [4], astronomy [5], economics [6] to experimental psychology [7]. The hysteresis is typically characterized by the presence of memory in its (dynamic) behaviour and has attracted the attention of scientists for its intrinsic complexity. The multitude of domains, where hysteresis can be found, has led most of the works in literature to describe it using phenomenological models which are rather independent of the specific process underlying it. In this regard, the Duhem model [8] is one of the well-known generic models of hysteresis. Its mathematical formulation encompasses many of other phenomenological models, for instance, the Dahl model, the Bouc-Wen model and the Maxwell-slip model [9]. Another large class of popular models is the Preisach models [9], [10] which will not be considered in this paper.

The Duhem model has been extensively studied in the literature and several mathematical properties have been established. Roughly speaking, the Duhem model maps input signals to output signals via switched nonlinear differential equations, where the switch signal depends on the sign of the derivative of its input signal. Mathematical properties of the resulting Duhem operator (with time-independent vector fields) have been presented in literature that include the existence and uniqueness of the solutions, as well as, monotonicity, semigroup and rate-independent properties. A thorough exposition of these properties and other fundamental mathematical properties can be found in [8], [11], [12]. Control systems properties, where the Duhem operator is feedback interconnected with other nonlinear systems, have been studied in the literature. For instance, the study of dissipativity in a class of Duhem operators is presented in [13]–[15] where the associated storage functions and supply rate functions depend on the specific hysteresis loops obtained from the Duhem models. In recent decades, attention has also been given to the convergent systems property [16] or consistency and strong-consistency [12], [17] of the Duhem model, where the output converges to a periodic signal when a periodic input signal is given. Such property in the literature of hysteresis is known as the accommodation property, as presented for instance in [18], which investigates the hysteresis modeling in ferromagnetic material. In this case, the phase plot of input and output signals will show loops that converge to a limit cycle around the so-called anhysteresis curve.

This convergent systems property has been shown for the semi-linear Duhem model [19] and for the Babuška's model [20], which is a class of the Duhem model where each vector field in the integro-differential equations can be expressed as the multiplication of two single variable functions. Moreover, [12] presents the analysis of the convergence properties of the LuGre friction model, which is based on the introduced concept of strong-consistency of the hysteresis map. Loosely speaking, strong-consistency refers to the property of the hysteresis map to approach a time-periodic when the input is periodic. Although the generality of this formulation is suitable for the study of rate-dependent hysteresis operators, it is beyond the scope of this work.

In this paper, we extend the aforementioned results to a class of Duhem models that can exhibit asymmetric butterfly loops. Here, the butterfly loops refer to presence of closed orbits with two or multiple loops in the input-output phase plot. While the standard hysteresis operators produce either counterclockwise or clockwise loops, the butterfly ones comprise of both clockwise and counterclockwise loops. The presence of butterfly loops has been shown and observed in practice for decades, e.g. in piezoactuator systems [21] and in magnetostrictive materials [22]. The first simple mathematical modeling, analysis and identification of hysteresis with butterfly loops is presented in [23], where a convex function is added to the output of standard hysteresis operator in order to enforce two inflection points to the standard loop and thereby creating butterfly loops. A general modeling and analysis of a butterfly hysteresis operator based on the Preisach model is

*This paper is based on research developed in the DSSC Doctoral Training Programme, co-funded through a Marie Skłodowska-Curie COFUND (DSSC 754315).

[1]M. A. Vasquez Beltran and B. Jayawardhana are with the Engineering and Technology Institute Groningen, Faculty of Science and Engineering, University of Groningen, 9747AG Groningen, The Netherlands {m.a.vasquez.beltran;b.jayawardhana} @rug.nl

[2]R. F. Peletier is with the Kapteyn Astronomical Institute, Faculty of Science and Engineering, University of Groningen, 9747AG Groningen, The Netherlands r.peletier@rug.nl

presented in [24], [25]. This class of Preisach operator was firstly reported in [26], where it is used to describe the shape memory property of a newly purposely-designed piezoelectric materials. This framework has been used in the development of a deformable mirror with high-density programmable actuators [27]–[29]. A MEMS mirror with programmable tilt whose actuators are modeled by Preisach hysteresis operators have also been studied in [30]. With the aim of providing an alternative modeling and analysis framework to describe the butterfly hysteresis loops of this piezoelectric material as well as other classes of actuators based on smart material or memory material, in this work, we study conditions that enable the Duhem model to exhibit multiple loops, including the butterfly loop. We note that the presence of multi-loops hysteresis behaviour in advanced materials has recently been shown in [31]. To the best of authors' knowledge, the modeling and analysis of a Duhem model that can exhibit multiple loops is still largely open.

As our first main contribution in the extension of previous results to the butterfly hysteresis operator using the Duhem model, we investigate the applicability of Babuška's conditions used in [20] as sufficient conditions for guaranteeing the convergence of the input-output phase plot to a closed orbit when the input signal is simple periodic[1] in Section III. These conditions correspond to the monotonicity of the vector fields in the Duhem model when the input argument is fixed. Using only these Babuška's conditions, we can relax the strong sign-definite assumption on these vector fields that are typically assumed in literature. Furthermore, we show that if we have strict monotonicity conditions then the closed orbit is unique for any initial value of the output. We have applied these conditions to the Bouc-Wen model and validated that in fact they are equivalent to some other known conditions in [32] that guarantee the BIBO stability of the model. In Section IV, we present our second main contribution, where we study a class of Duhem models whose vector fields are sign-indefinite but satisfy the aforementioned Babuška's conditions. Under some additional mild assumptions on the vector fields, we show that the input-output phase plot of this Duhem model converges to a closed orbit with two or more loops, for example, it can exhibit a butterfly loop. We remark that the conditions presented in this section focus on the phenomenological description of the butterfly hysteresis loops and on finding vector functions f_1 and f_2 that have specific physical interpretation. Such characterisation of Duhem models that can produce butterfly hysteresis loops is, to the best author's knowledge, still an open problem. At the end of Section IV we provide illustrative examples of this class of Duhem models using simple vector functions composed of polynomial.

II. PRELIMINARIES

Notation. We denote by $C(U,Y)$, $AC(U,Y)$, $C_{\mathrm{pw}}(U,Y)$ the spaces of continuous, absolute continuous, and piece-wise continuous functions $f : U \to Y$, respectively. We denote $\mathbb{R}_+ := [0,\infty)$. Moreover, we call a function $f : U \to Y$ monotonically increasing (resp. decreasing) $u_1 < u_2$ implies $f(u_1) \leq f(u_2)$ (resp. $f(u_1) \geq f(u_2)$), and strictly monotonically increasing (resp. decreasing) if the inequality is strict.

We define the next two auxiliary operators which are used throughout this work. The right-shift operator $\mathcal{S}_\tau \colon AC(\mathbb{R}_+,\mathbb{R}) \to AC(\mathbb{R}_+,\mathbb{R})$ parameterized by $\tau \in \mathbb{R}$ is defined by

$$[\mathcal{S}_\tau(v)](t) := v(t+\tau). \tag{1}$$

The right-continuation operator $\mathcal{R}_\tau \colon AC(\mathbb{R}_+,\mathbb{R}) \to AC(\mathbb{R}_+,\mathbb{R})$ parameterized by $\tau \in \mathbb{R}_+$ is defined by

$$[\mathcal{R}_\tau(v)](t) := \begin{cases} v(t) & \text{if } t \in [0,\tau], \\ v(\tau) & \text{if } t \in (\tau,\infty). \end{cases} \tag{2}$$

The Duhem hysteresis operator operator is a mapping $\Phi \colon AC(\mathbb{R}_+,\mathbb{R}) \times \mathbb{R} \to AC(\mathbb{R}_+,\mathbb{R})$ such that $y = \Phi(u,y_0)$ satisfies

$$\begin{aligned} \dot{y}(t) &= \begin{cases} f_1(u(t),y(t))\dot{u}, & \text{if } \dot{u}(t) \geq 0, \\ f_2(u(t),y(t))\dot{u}, & \text{if } \dot{u}(t) < 0, \end{cases} \\ y(0) &= y_0, \end{aligned} \tag{3}$$

at almost every $t \geq 0$ and with $f_1, f_2 \in C^0(\mathbb{R}^2,\mathbb{R})$. Given an arbitrary input $u \in AC(\mathbb{R}_+,\mathbb{R})$ and initial condition $y_0 \in \mathbb{R}$, the existence and uniqueness of $y \in AC(\mathbb{R}_+,\mathbb{R})$ satisfying (3) at almost every $t \in [0,T]$ with $T > 0$ is studied in [9], [11] and guaranteed when f_1 and f_2 satisfy

$$(f_1(\upsilon,\gamma_1) - f_1(\upsilon,\gamma_2))(\gamma_1-\gamma_2) \leq \quad \lambda_1(u)(\gamma_1-\gamma_2)^2, \tag{4}$$

$$(f_2(\upsilon,\gamma_1) - f_2(\upsilon,\gamma_2))(\gamma_1-\gamma_2) \geq -\lambda_2(u)(\gamma_1-\gamma_2)^2, \tag{5}$$

for every $\upsilon,\gamma_1,\gamma_2 \in \mathbb{R}$ and some for non-negative functions $\lambda_1,\lambda_2 \in C(\mathbb{R},\mathbb{R}_+)$.

An important property of the Duhem operator Φ as defined in (3) is that it is rate-independent. In other words, for every $\phi \in C(\mathbb{R}_+,\mathbb{R}_+)$ such that $\phi(0) = 0$, increasing and radially unbounded (i.e. $\phi(t) \to \infty$ as $t \to \infty$) we have

$$\big[\Phi(u \circ \phi, y_0)\big](t) = [\Phi(u,y_0) \circ \phi](t).$$

Moreover, following the work of [11], we consider hysteresis operator that satisfies the semi-group property, which means that if $y = \Phi(u,y_0)$ then

$$\mathcal{S}_\tau(\Phi(u,y_0)) = \Phi(\mathcal{S}_\tau(u),\mathcal{S}_\tau(y)).$$

Throughout this work we assume that the implicit function $\upsilon \mapsto \{\gamma \in \mathbb{R} \mid f_1(\upsilon,\gamma) - f_2(\upsilon,\gamma) = 0\}$ admits an explicit solution

$$\gamma = \alpha(\upsilon) \tag{6}$$

with $\alpha \in C^0(\mathbb{R},\mathbb{R})$, which we call the *anhysteresis function* and the corresponding curve (generated by α) given by

$$\mathcal{A} = \big\{(\upsilon,\gamma) \in \mathbb{R}^2 \mid \gamma = \alpha(\upsilon)\big\}, \tag{7}$$

is called the *anhysteresis curve*. By definition, the curve $\mathcal{A}$ divides the input-output plane into two regions where $f_1(\upsilon,\gamma_1) - f_2(\upsilon,\gamma_1) \geq 0$ whenever $\gamma_1 \geq \gamma = \alpha(\upsilon)$, and $f_1(\upsilon,\gamma_1) - f_2(\upsilon,\gamma_1) \leq 0$ whenever $\gamma_1 \leq \gamma = \alpha(\upsilon)$.

[1] A periodic signal is called simple if it admits only one maximum and one minimum within its periodic interval.

III. THE DUHEM OPERATOR ACCOMMODATION PROPERTY

As briefly described in the Introduction, the accommodation property of the Duhem operator Φ refers to the property where the input-output phase plot always converges to a periodic closed orbit when the input signal is periodic [18]. In this section, we formally study this property and prove that when the input is periodic with a single maximum and a single minimum in its periodic interval, the input-output phase plot approaches a unique periodic closed-loop which revolves in a neighborhood of the anhysteresis curve $\mathcal{A}$. We begin studying the input-output phase plot produced by the application of monotonic inputs and then we extend our analysis to periodic inputs. For simplicity of notation, in what follows we use $Y_u\colon \mathbb{R}_+ \times \mathbb{R} \to \mathbb{R}$, which we define by

$$Y_u(t,y_0) := [\Phi(u,y_0)](t),$$

to refer to the output of the Duhem operator Φ parameterized by the input signal u and with the time t and initial condition y_0 as independent variables.

A. The Duhem operator with monotonic inputs

Let $u_+ \in AC(\mathbb{R}_+,\mathbb{R})$ be an input which is monotonically increasing in $[0,\infty)$ and consider a sub-interval $[0,\tau_1]$ with $\tau_1 > 0$ such that $u(0) = \upsilon_{\min} < \upsilon_{\max} = u(\tau_1)$. Since the Duhem operator Φ defined with (3) is rate-independent as shown in [8], [11], [19], for every $t \in [0,\tau_1]$ we have that

$$\begin{aligned} Y_{u_+}(t,y_0) - y_0 &= \int_0^t f_1\left(u_+(\tau),\ Y_{u_+}(\tau,y_0)\right)\ \dot{u}(\tau)\ \mathrm{d}\tau \\ &= \int_{\upsilon_{\min}}^{u_+(t)} f_1\left(\upsilon, \mathcal{Y}_{u_+}(\upsilon,y_0)\right)\ \mathrm{d}\upsilon \\ &= \mathcal{Y}_{u_+}(u_+(t),y_0) - \mathcal{Y}_{u_+}(\upsilon_{\min},y_0) \end{aligned} \tag{8}$$

where

$$\mathcal{Y}_{u_+}\colon [\upsilon_{\min},\upsilon_{\max}] \times \mathbb{R} \to \mathbb{R}$$

is the parameterization of the corresponding solution $Y_{u_+}(t,y_0)$ with the instantaneous value of the input u_+ and the initial condition y_0 as independent variables (i.e. $\mathcal{Y}_{u_+}(u_+(t),y_0) = Y_{u_+}(t,y_0)$ for every $t \in [0,\tau_1]$).

Analogously, let $u_- \in AC(\mathbb{R}_+,\mathbb{R})$ be an input which is monotonically decreasing in $[0,\infty)$ and consider a sub-interval $[0,\tau_2]$ with $\tau_2 > 0$ such that $u(0) = \upsilon_{\max} > \upsilon_{\min} = u(\tau_2)$. By the rate-independent property of the Duhem operator, we have that, for every $t \in [0,\tau_2]$,

$$\begin{aligned} Y_{u_-}(t,y_0) - y_0 &= \int_0^t f_2\left(u_-(\tau),\ Y_{u_-}(\tau,y_0)\right)\ \dot{u}(\tau)\ \mathrm{d}\tau \\ &= \int_{\upsilon_{\max}}^{u_-(t)} f_2\left(\upsilon, \mathcal{Y}_{u_-}(\upsilon,y_0)\right)\ \mathrm{d}\upsilon \\ &= \mathcal{Y}_{u_-}(u_-(t),y_0) - \mathcal{Y}_{u_-}(\upsilon_{\max},y_0) \end{aligned} \tag{9}$$

where in this case

$$\mathcal{Y}_{u_-}\colon [\upsilon_{\min},\upsilon_{\max}] \times \mathbb{R} \to \mathbb{R}$$

is the parameterization of the corresponding solution $Y_{u_-}(t,y_0)$ with the instantaneous value of the input u_- and the initial condition y_0 as independent variables (i.e. $\mathcal{Y}_{u_-}(u_-(t),y_0) = Y_{u_-}(t,y_0)$ for every $t \in [0,\tau_2]$).

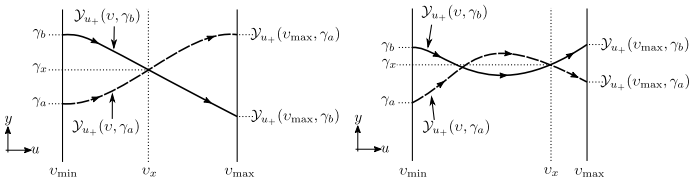

(a) Contradiction of case *a)* in Lemma 3.1.

(b) Contradiction of case *b)* in Lemma 3.1.

Figure 1: Illustration of non-possible intersection between solutions in the input-output phase plot as shown in Lemma 3.1 corresponding to $\mathcal{Y}_{u_+}$. The one for $\mathcal{Y}_{u_-}$ follows in a similar fashion.

In what follows, we present a series of auxiliary lemmas necessary to prove the accommodation property. Firstly, using the parameterizations $\mathcal{Y}_{u_+}$ and $\mathcal{Y}_{u_-}$ of the output, we state formally in the first lemma that two input-output phase plots obtained with the same monotonic input but from different initial conditions never cross each other.

Lemma 3.1: The next statements are true.

a) If two initial conditions satisfy $\gamma_a \le \gamma_b$, then we have

$$\begin{aligned} \mathcal{Y}_{u_+}(\upsilon,\gamma_a) &\le \mathcal{Y}_{u_+}(\upsilon,\gamma_b), \\ \mathcal{Y}_{u_-}(\upsilon,\gamma_a) &\le \mathcal{Y}_{u_-}(\upsilon,\gamma_b), \end{aligned}$$

for every $\upsilon \in [\upsilon_{\min},\upsilon_{\max}]$.

b) If we have that

$$\begin{aligned} &\mathcal{Y}_{u_+}(\upsilon_{\max},\gamma_a) < \mathcal{Y}_{u_+}(\upsilon_{\max},\gamma_b) \\ &\left(\text{resp. } \mathcal{Y}_{u_-}(\upsilon_{\min},\gamma_a) < \mathcal{Y}_{u_-}(\upsilon_{\min},\gamma_b)\right), \end{aligned}$$

then

$$\begin{aligned} &\mathcal{Y}_{u_+}(\upsilon,\gamma_a) < \mathcal{Y}_{u_+}(\upsilon,\gamma_b) \\ &\left(\text{resp. } \mathcal{Y}_{u_-}(\upsilon,\gamma_a) < \mathcal{Y}_{u_-}(\upsilon,\gamma_b)\right), \end{aligned}$$

for every $\upsilon \in [\upsilon_{\min},\upsilon_{\max}]$.

PROOF: In what follows, we prove both statements for $\mathcal{Y}_{u_+}$ by contradiction. The proof for $\mathcal{Y}_{u_-}$ can be obtained in a similar way by vis-a-vis arguments and it is omitted.

Part a) Let $\gamma_a \le \gamma_b$ and assume that $\mathcal{Y}_{u_+}(\upsilon_c,\gamma_a) > \mathcal{Y}_{u_+}(\upsilon_c,\gamma_b)$ for some $\upsilon_c \in [\upsilon_{\min},\upsilon_{\max}]$.

Let $\tau_c \in [0,\tau_1]$ be a time instance such that $\mathcal{Y}_{u_+}(\upsilon_c,\gamma_a) = Y_{u_+}(\tau_c,\gamma_a) > Y_{u_+}(\tau_c,\gamma_b) = \mathcal{Y}_{u_+}(\upsilon_c,\gamma_b)$.

By continuity of $\mathcal{Y}_{u_+}$, there exists $\upsilon_x \in [\upsilon_{\min},\upsilon_c)$ such that $\gamma_x = \mathcal{Y}_{u_+}(\upsilon_x,\gamma_a) = \mathcal{Y}_{u_+}(\upsilon_x,\gamma_b)$ (see Fig. 1a). Let $\tau_x \in [0,\tau_c)$ be a time instance such that $\gamma_x = Y_{u_+}(\tau_x,\gamma_a) = Y_{u_+}(\tau_x,\gamma_b)$.

We can create a right-shifted input $u_s = \mathcal{S}_{\tau_x}(u_+)$ and note that by the semi-group property of the Duhem operator we must have that

$$Y_{u_+}(t+\tau_x,\gamma_a) = Y_{u_s}(t,\gamma_x) = Y_{u_+}(t+\tau_x,\gamma_b)$$

for every $t \in [0,\tau_1-\tau_x]$, which implies a contradiction to the uniqueness of solution Y_{u_s} since

$$Y_{u_+}(\tau_c,\gamma_a) > Y_{u_+}(\tau_c,\gamma_b).$$

Therefore, $\mathcal{Y}_{u_+}(\upsilon,\gamma_a) \le \mathcal{Y}_{u_+}(\upsilon,\gamma_b)$ for every $\upsilon \in [\upsilon_{\min},\upsilon_{\max}]$.

Part b) Let $\mathcal{Y}_{u_+}(\upsilon_{\max},\gamma_a) < \mathcal{Y}_{u_+}(\upsilon_{\max},\gamma_b)$ and assume that $\gamma_x = \mathcal{Y}_{u_+}(\upsilon_x,\gamma_a) = \mathcal{Y}_{u_+}(\upsilon_x,\gamma_b)$ for some $\upsilon_x \in [\upsilon_{\min},\upsilon_{\max})$ (see Fig. 1b). Letting $\tau_x \in [0,\tau_1)$ be a time instance such that $\gamma_x = Y_{u_+}(\tau_x,\gamma_a) = Y_{u_+}(\tau_x,\gamma_b)$ and creating right-shifted input $u_s = \mathcal{S}_{\tau_x}(u_+)$ we can obtain the same contradiction as in *Part a)*. Therefore, $\mathcal{Y}_{u_+}(\upsilon,\gamma_a) < \mathcal{Y}_{u_+}(\upsilon,\gamma_b)$ for every $\upsilon \in [\upsilon_{\min},\upsilon_{\max}]$

□

B. The Duhem operator with a periodic input

We can now analyze the behavior of the Duhem operator Φ when the applied input signal is simple periodic. For this, let $u_p \in AC(\mathbb{R}_+,\mathbb{R})$ be a periodic input with period $T > 0$ and with one minimum and one maximum $\upsilon_{\min} < \upsilon_{\max}$ in its periodic interval. Without loss of generality, we assume that $u_p(0) = \upsilon_{\min}$ and $u_p(t_1) = \upsilon_{\max}$ for some $t_1 \in (0,T)$. In other words, $0 < t_1 < T$ is a monotonic partition of $[0,T]$. We can split u_p into its two monotonic intervals using the right-shift and right-continuation operators (1) and (2), which are formalized using two functions $u_{p+},u_{p-} \in AC(\mathbb{R}_+,\mathbb{R})$ given by

$$u_{p+} = \mathcal{R}_{t_1}(u_p),$$
$$u_{p-} = \mathcal{S}_{t_1}(\mathcal{R}_T(u_p)),$$

whose corresponding outputs when applied to the Duhem operator are given by $Y_{u_{p+}}(t,\gamma)$ and $Y_{u_{p-}}(t,\zeta)$ for some initial conditions $\gamma,\zeta \in \mathbb{R}$.

Following the same argumentation as before to obtain (8) and (9), we can parameterize $Y_{u_{p+}}(t,\gamma)$ and $Y_{u_{p-}}(t,\zeta)$ by two mappings

$$\mathcal{Y}_{u_{p+}} \colon [\upsilon_{\min},\upsilon_{\max}] \times \mathbb{R} \to \mathbb{R},$$
$$\mathcal{Y}_{u_{p-}} \colon [\upsilon_{\min},\upsilon_{\max}] \times \mathbb{R} \to \mathbb{R},$$

respectively, where the instantaneous values of the inputs u_{p+} and u_{p-}, and initial conditions γ and ζ are the independent variables.

For arbitrary $\gamma_0 \in \mathbb{R}$, let us define two sequences $(\zeta_n)_{n\in\mathbb{N}_0}$ and $(\gamma_n)_{n\in\mathbb{N}_0}$ recursively by

$$\zeta_n := \mathcal{Y}_{u_{p+}}(\upsilon_{\max},\gamma_n), \tag{10}$$
$$\gamma_{n+1} := \mathcal{Y}_{u_{p-}}(\upsilon_{\min},\zeta_n). \tag{11}$$

Note then that making $\gamma_0 = y_0$, the output $Y_{u_p}(t,y_0)$ can be constructed recursively by

$$Y_{u_p}(t,y_0) = \begin{cases} \mathcal{Y}_{u_{p+}}(u_p(t),\gamma_n), & \text{if} \quad nT \le t < t_1 + nT, \\ \mathcal{Y}_{u_{p-}}(u_p(t),\zeta_n), & \text{if } t_1 + nT \le t < (n+1)T, \end{cases}$$

where $n \in \mathbb{N}_0$ and $t_1 > 0$ is such that $0 < t_1 < T$ is a monotonic partition of $[0,T]$. Therefore, we study the convergence of the solution Y_{u_p} to a periodic solution using these sequences.

The next three lemmas present properties of the sequences $(\zeta_n)_{n\in\mathbb{N}_0}$ and $(\gamma_n)_{n\in\mathbb{N}_0}$ generated by the recursive composition of the function $\mathcal{Y}_{u_{p+}}$ and $\mathcal{Y}_{u_{p-}}$ that will be used in the proof of the main result of this section.

Lemma 3.2: Let $\gamma_0 \in \mathbb{R}$. The sequences $(\zeta_n)_{n\in\mathbb{N}_0}$ and $(\gamma_n)_{n\in\mathbb{N}_0}$ generated by (10) and (11) are monotonic in the same direction (i.e. both increasing or both decreasing).

PROOF: By induction, let $\gamma_i \ge \gamma_{i+1}$ and note that by Lemma 3.1, we have

$$\zeta_i = \mathcal{Y}_{u_{p+}}(\upsilon_{\max},\gamma_i) \ge \mathcal{Y}_{u_{p+}}(\upsilon_{\max},\gamma_{i+1}) = \zeta_{i+1}$$
$$\gamma_i = \mathcal{Y}_{u_{p-}}(\upsilon_{\min},\zeta_i), \ge \mathcal{Y}_{u_{p-}}(\upsilon_{\min},\zeta_{i+1}) = \gamma_{i+2},$$

which proves that both sequences are increasing. Reversing all previous inequalities proves that both sequences are decreasing. □

Lemma 3.3: Let $\gamma_0 \in \mathbb{R}$ and consider the sequences $(\zeta_n)_{n\in\mathbb{N}_0}$ and $(\gamma_n)_{n\in\mathbb{N}_0}$ generated by (10) and (11). Then the next statements are true.

a) If $\gamma_i = \gamma_{i+1}$ for some $i \in \mathbb{N}_0$ then for every $k \ge i$ we have
$$\zeta_k = \zeta_{k+1} \qquad \text{and} \qquad \gamma_{k+1} = \gamma_{k+2}.$$

b) If $\zeta_j = \zeta_{j+1}$ for some $j \in \mathbb{N}_0$ then for every $k \ge j$ we have
$$\gamma_{k+1} = \gamma_{k+2} \qquad \text{and} \qquad \zeta_{k+1} = \zeta_{k+2}.$$

PROOF: Let $\gamma_i = \gamma_{i+1}$ and note that the uniqueness of solution $Y_{u_{p+}}$ implies $\mathcal{Y}_{u_{p+}}(\upsilon,\gamma_i) = \mathcal{Y}_{u_{p+}}(\upsilon,\gamma_{i+1})$ for every $\upsilon \in [\upsilon_{\min},\upsilon_{\max}]$, and consequently $\zeta_i = \mathcal{Y}_{u_{p+}}(\upsilon_{\max},\gamma_i) = \mathcal{Y}_{u_{p+}}(\upsilon_{\max},\gamma_{i+1}) = \zeta_{i+1}$. Therefore, we have that

$$\gamma_i = \gamma_{i+1} \qquad \Rightarrow \qquad \zeta_i = \zeta_{i+1}.$$

Similarly, when $\zeta_j = \zeta_{j+1}$, the uniqueness of solution $Y_{u_{p-}}$ implies $\mathcal{Y}_{u_{p-}}(\upsilon,\zeta_j) = \mathcal{Y}_{u_{p-}}(\upsilon,\zeta_{j+1})$ for every $\upsilon \in [\upsilon_{\min},\upsilon_{\max}]$, and consequently $\gamma_{j+1} = \mathcal{Y}_{u_{p+}}(\upsilon_{\min},\zeta_j) = \mathcal{Y}_{u_{p-}}(\upsilon_{\min},\zeta_{j+1}) = \gamma_{j+2}$. Thus we have that

$$\zeta_j = \zeta_{j+1} \qquad \Rightarrow \qquad \gamma_{j+1} = \gamma_{j+2}.$$

It follows that combining both implications proves both statements. □

Lemma 3.4: Let $\gamma_0 \in \mathbb{R}$ and consider the sequences $(\zeta_n)_{n\in\mathbb{N}_0}$ and $(\gamma_n)_{n\in\mathbb{N}_0}$ generated by (10) and (11). The sequence $(\zeta_n)_{n\in\mathbb{N}_0}$ is unbounded if and only if $(\gamma_n)_{n\in\mathbb{N}_0}$ is unbounded. Moreover, when they are unbounded, they are strictly monotonic in the same direction (i.e. both strictly increasing or both strictly decreasing).

PROOF: To prove the if part, let $(\gamma_n)_{n\in\mathbb{N}_0}$ be unbounded and note that by Lemma 3.2 we have that both sequences $(\gamma_n)_{n\in\mathbb{N}_0}$ and $(\zeta_n)_{n\in\mathbb{N}_0}$ are monotonic in the same direction. Moreover, by Lemma 3.3, assuming that $\gamma_i = \gamma_{i+1}$ or $\zeta_j = \zeta_{j+1}$ for some $i,j \in \mathbb{N}_0$ implies that $(\gamma_n)_{n\in\mathbb{N}_0}$ is not unbounded, which is a contradiction. Therefore $(\zeta_n)_{n\in\mathbb{N}_0}$ is also unbounded and both are strictly monotonic.

To prove the only if part, let $(\zeta_n)_{n\in\mathbb{N}_0}$ be unbounded and note that by Lemma 3.2 we have that both sequences $(\gamma_n)_{n\in\mathbb{N}_0}$

and $(\zeta_n)_{n\in\mathbb{N}_0}$ are monotonic in the same direction. Moreover, by Lemma 3.3, assuming that $\gamma_i = \gamma_{i+1}$ or $\zeta_j = \zeta_{j+1}$ for some $i, j \in \mathbb{N}_0$ implies that $(\zeta_n)_{n\in\mathbb{N}_0}$ is not unbounded, which is a contradiction. Therefore $(\gamma_n)_{n\in\mathbb{N}_0}$ is also unbounded and both are strictly monotonic. □

In the next two propositions, we introduce the main results of this section where sufficient conditions are presented such that the sequences $(\gamma_n)_{n\in\mathbb{N}_0}$ and $(\zeta_n)_{n\in\mathbb{N}_0}$ generated by (10) and (11) are convergent. We remark that if the sequences $(\zeta_n)_{n\in\mathbb{N}_0}$ and $(\gamma_n)_{n\in\mathbb{N}_0}$ are convergent to some pair $\gamma_* \in \mathbb{R}$ and $\zeta_* \in \mathbb{R}$, respectively, then due to the continuity and uniqueness of solution of the Duhem operator we must have that

$$\begin{aligned} \mathcal{Y}_{u_{p+}}(\upsilon_{\max}, \gamma_*) &= \zeta_*, \\ \mathcal{Y}_{u_{p-}}(\upsilon_{\min}, \zeta_*) &= \gamma_*, \end{aligned}$$

and consequently both parameterized solutions $\mathcal{Y}_{u_{p+}}(\upsilon, \gamma_*)$ and $\mathcal{Y}_{u_{p-}}(\upsilon, \zeta_*)$ form a periodic closed orbit in the phase plot. With the first proposition we present a pair of inequalities that ensure the convergence to some periodic orbit. These inequalities have been previously presented in [20] and are used together with other set of conditions to prove the convergence of the output to a periodic function for a specific version of the Duhem model known as Babuška's model. We show that only these two conditions are sufficient to ensure the convergence of the output to a periodic function in the scalar rate-independent Duhem model. Subsequently, with the second proposition we show that the strict versions of the inequalities ensure the uniqueness of the pair $\gamma_* \in \mathbb{R}$ and $\zeta_* \in \mathbb{R}$ and consequently the uniqueness of the closed periodic orbit.

Proposition 3.5: If the functions f_1 and f_2 in (3) satisfy

$$(f_1(\upsilon, \gamma_1) - f_1(\upsilon, \gamma_2))(\gamma_1 - \gamma_2) \leq 0, \tag{12}$$

$$(f_2(\upsilon, \gamma_1) - f_2(\upsilon, \gamma_2))(\gamma_1 - \gamma_2) \geq 0, \tag{13}$$

for every $\gamma_1 \neq \gamma_2$ and $\upsilon \in \mathbb{R}$, then for every $\gamma_0 \in \mathbb{R}$ the sequences $(\zeta_n)_{n\in\mathbb{N}_0}$ and $(\gamma_n)_{n\in\mathbb{N}_0}$ generated by (10) and (11) are convergent.

Prior to proving the proposition above, we need the following technical lemma.

Lemma 3.6: Suppose that (12) and (13) hold with divergent sequences $(\zeta_n)_{n\in\mathbb{N}_0}$ and $(\gamma_n)_{n\in\mathbb{N}_0}$ generated by (10) and (11), both of which are unbounded and strictly monotonic in the same direction according to Lemma 3.4. Then, for fixed $\upsilon \in [\upsilon_{\min}, \upsilon_{\max}]$, the sequences

$$\left(\mathcal{Y}_{u_{p+}}(\upsilon, \gamma_n)\right)_{n\in\mathbb{N}_0} \qquad \text{and} \qquad \left(\mathcal{Y}_{u_{p-}}(\upsilon, \zeta_n)\right)_{n\in\mathbb{N}_0},$$

are also unbounded and strictly monotonic in the same direction as the sequences $(\zeta_n)_{n\in\mathbb{N}_0}$ or $(\gamma_n)_{n\in\mathbb{N}_0}$.

PROOF OF LEMMA 3.6: From (8), we can obtain

$$\begin{aligned} \mathcal{Y}_{u_{p+}}(\upsilon, \gamma_i) - \mathcal{Y}_{u_{p+}}(\upsilon, \gamma_{i-1}) = \\ \int_{\upsilon_{\min}}^{\upsilon} \left\{ f_1\left(\nu, \mathcal{Y}_{u_{p+}}(\nu, \gamma_i)\right) - f_1\left(\nu, \mathcal{Y}_{u_{p+}}(\nu, \gamma_{i-1})\right) \right\} \mathrm{d}\nu \\ + \gamma_i - \gamma_{i-1}. \end{aligned} \tag{14}$$

Moreover, we have that

$$\zeta_i = \int_{\upsilon_{\min}}^{\upsilon_{\max}} f_1\left(\nu, \mathcal{Y}_{u_{p+}}(\nu, \gamma_i)\right) \mathrm{d}\nu + \gamma_i.$$

Therefore, we can solve the previous expression for γ_i and γ_{i-1} and replace both into (14) to obtain

$$\begin{aligned} \mathcal{Y}_{u_{p+}}(\upsilon, \gamma_i) - \mathcal{Y}_{u_{p+}}(\upsilon, \gamma_{i-1}) = \\ - \int_{\upsilon}^{\upsilon_{\max}} \left\{ f_1\left(\nu, \mathcal{Y}_{u_{p+}}(\nu, \gamma_i)\right) - f_1\left(\nu, \mathcal{Y}_{u_{p+}}(\nu, \gamma_{i-1})\right) \right\} \mathrm{d}\nu \\ + \zeta_i - \zeta_{i-1}, \end{aligned}$$

and by (12), the integrand in the previous expression is negative or zero when $\gamma_i > \gamma_{i-1}$ and positive or zero when $\gamma_i < \gamma_{i-1}$. Consequently, for every $\upsilon \in [\upsilon_{\min}, \upsilon_{\max}]$ we have

$$\begin{aligned} \mathcal{Y}_{u_{p+}}(\upsilon, \gamma_i) &\geq \zeta_i - \zeta_{i-1} + \mathcal{Y}_{u_{p+}}(\upsilon, \gamma_{i-1}), \quad \text{when } \gamma_i > \gamma_{i-1}, \\ \mathcal{Y}_{u_{p+}}(\upsilon, \gamma_i) &\leq \zeta_i - \zeta_{i-1} + \mathcal{Y}_{u_{p+}}(\upsilon, \gamma_{i-1}), \quad \text{when } \gamma_i < \gamma_{i-1}, \end{aligned}$$

and fixing the terms γ_{i-1} and ζ_{i-1}, then it follows that $\mathcal{Y}_{u_{p+}}(\upsilon, \gamma_i)$ is unbounded in the same direction than ζ_i.

In a similar way, from (9) we can obtain

$$\begin{aligned} \mathcal{Y}_{u_{p-}}(\upsilon, \zeta_i) - \mathcal{Y}_{u_{p-}}(\upsilon, \zeta_{i-1}) = \\ - \int_{\upsilon}^{\upsilon_{\max}} \left\{ f_2\left(\nu, \mathcal{Y}_{u_{p-}}(\nu, \zeta_i)\right) - f_2\left(\nu, \mathcal{Y}_{u_{p-}}(\nu, \zeta_{i-1})\right) \right\} \mathrm{d}\nu \\ + \zeta_i - \zeta_{i-1}. \end{aligned} \tag{15}$$

Again, note that we have

$$\gamma_i = - \int_{\upsilon_{\min}}^{\upsilon_{\max}} f_2\left(\nu, \mathcal{Y}_{u_{p-}}(\nu, \zeta_{i-1})\right) \mathrm{d}\nu + \zeta_{i-1}.$$

Therefore, we can solve the previous expression for ζ_{i-1} and ζ_i and replace both into (15) to obtain

$$\begin{aligned} \mathcal{Y}_{u_{p-}}(\upsilon, \zeta_i) - \mathcal{Y}_{u_{p-}}(\upsilon, \zeta_{i-1}) = \\ \int_{\upsilon_{\min}}^{\upsilon} \left\{ f_2\left(\nu, \mathcal{Y}_{u_{p-}}(\nu, \zeta_i)\right) - f_2\left(\nu, \mathcal{Y}_{u_{p-}}(\nu, \zeta_{i-1})\right) \right\} \mathrm{d}\nu \\ + \gamma_{i+1} - \gamma_i, \end{aligned}$$

and by (13), the integrand in the previous expression is positive or zero when $\zeta_i > \zeta_{i-1}$ and negative or zero when $\zeta_i < \zeta_{i-1}$. Consequently, for every $\upsilon \in [\upsilon_{\min}, \upsilon_{\max}]$ we have

$$\begin{aligned} \mathcal{Y}_{u_{p-}}(\upsilon, \zeta_i) &\geq \gamma_{i+1} - \gamma_i + \mathcal{Y}_{u_{p-}}(\upsilon, \zeta_{i-1}), \quad \text{when } \zeta_i > \zeta_{i-1}, \\ \mathcal{Y}_{u_{p-}}(\upsilon, \zeta_i) &\leq \gamma_{i+1} - \gamma_i + \mathcal{Y}_{u_{p-}}(\upsilon, \zeta_{i-1}), \quad \text{when } \zeta_i < \zeta_{i-1}, \end{aligned}$$

and fixing the terms γ_i and ζ_{i-1}, then it follows that $\mathcal{Y}_{u_{p-}}(\upsilon, \zeta_i)$ is unbounded in the same direction than γ_{i+1}. □

PROOF OF PROPOSITION 3.5:
It follows from (8) and (9) that the difference between two consecutive elements in $(\gamma_n)_{n\in\mathbb{N}_0}$ is given by

$$\gamma_{i+1} - \gamma_i = \int_{\upsilon_{\min}}^{\upsilon_{\max}} \left\{ f_1\left(\nu, \mathcal{Y}_{u_{p+}}(\upsilon, \gamma_i)\right) - f_2\left(\upsilon, \mathcal{Y}_{u_{p-}}(\upsilon, \zeta_i)\right) \right\} \mathrm{d}\upsilon \tag{16}$$

Moreover, since by the definition of anhysteresis function α, we have $f_1(\upsilon, \alpha(\upsilon)) = f_2(\upsilon, \alpha(\upsilon))$ for every $\upsilon \in [\upsilon_{\min}, \upsilon_{\max}]$,

then we can add and subtract these terms inside the integral and obtain

$$\gamma_{i+1}-\gamma_i = \int_{\upsilon_{\min}}^{\upsilon_{\max}} \left\{ f_1\left(\nu, \mathcal{Y}_{u_{p+}}(\nu,\gamma_i)\right) - f_1\left(\nu,\alpha(\upsilon)\right)\right\} \mathrm{d}\nu - \int_{\upsilon_{\min}}^{\upsilon_{\max}} \left\{ f_2\left(\nu, \mathcal{Y}_{u_{p-}}(\nu,\zeta_i)\right) - f_2\left(\nu,\alpha(\upsilon)\right)\right\} \mathrm{d}\nu. \tag{17}$$

We prove the proposition by contradiction. Assume that any of the sequences $(\zeta_n)_{n\in\mathbb{N}_0}$ or $(\gamma_n)_{n\in\mathbb{N}_0}$ is not convergent. Thus by Lemmas 3.2, 3.3 and 3.4 both are unbounded and strictly monotonic in the same direction.

On the one hand, if both are strictly increasing, then by Lemmas 3.1 and 3.6 we can find two pairs $\gamma_i < \gamma_{i+1}$ and $\zeta_i < \zeta_{i+1}$ such that both $\mathcal{Y}_{u_{p+}}(\upsilon,\gamma_i)$ and $\mathcal{Y}_{u_{p-}}(\upsilon,\zeta_i)$ lie completely above the anhysteresis curve $\mathcal{A}$ given in (7) (see Fig. 2a). In other words, there exists $i\in\mathbb{N}_0$ such that

$$\mathcal{Y}_{u_{p+}}(\upsilon,\gamma_i) > \alpha(\upsilon) \quad \text{and} \quad \mathcal{Y}_{u_{p-}}(\upsilon,\zeta_i) > \alpha(\upsilon),$$

for every $\upsilon\in[\upsilon_{\min},\upsilon_{\max}]$, where α is the anhysteresis function (6). It follows also from (12) and (13) that we have

$$f_1\left(\upsilon,\mathcal{Y}_{u_{p+}}(\upsilon,\gamma_i)\right) - f_1\left(\upsilon,\alpha(\upsilon)\right) \le 0,$$
$$f_2\left(\upsilon,\mathcal{Y}_{u_{p-}}(\upsilon,\zeta_i)\right) - f_2\left(\upsilon,\alpha(\upsilon)\right) \ge 0,$$

for every $\upsilon\in[\upsilon_{\min},\upsilon_{\max}]$. Consequently the right term of (17) is negative or zero, which is a contradiction since by assumption the sequence is strictly increasing and $\gamma_{i+1}-\gamma_i>0$ for every $i\in\mathbb{N}_0$.

On the other hand, if both sequences $(\zeta_n)_{n\in\mathbb{N}_0}$ and $(\gamma_n)_{n\in\mathbb{N}_0}$ are strictly decreasing, then also Lemmas 3.1 and 3.6 we can find two pairs $\gamma_i > \gamma_{i+1}$ and $\zeta_i > \zeta_{i+1}$ such that both $\mathcal{Y}_{u_{p+}}(\upsilon,\gamma_i)$ and $\mathcal{Y}_{u_{p-}}(\upsilon,\zeta_i)$ lie completely below the anhysteresis curve $\mathcal{A}$ (see Fig. 2b) and we have

$$\mathcal{Y}_{u_{p+}}(\upsilon,\gamma_i) < \alpha(\upsilon) \quad \text{and} \quad \mathcal{Y}_{u_{p-}}(\upsilon,\zeta_i) < \alpha(\upsilon),$$

for every $\upsilon\in[\upsilon_{\min},\upsilon_{\max}]$ and some $i\in\mathbb{N}_0$. Similar as before, from (12) and (13) we have that

$$f_1\left(\upsilon,\mathcal{Y}_{u_{p+}}(\upsilon,\gamma_i)\right) - f_1\left(\upsilon,\alpha(\upsilon)\right) \ge 0,$$
$$f_2\left(\upsilon,\mathcal{Y}_{u_{p-}}(\upsilon,\zeta_i)\right) - f_2\left(\upsilon,\alpha(\upsilon)\right) \le 0,$$

for every $\upsilon\in[\upsilon_{\min},\upsilon_{\max}]$. Consequently, the right term of (17) is positive or zero, which is a contradiction since by assumption the sequence is strictly decreasing and $\gamma_{i+1}-\gamma_i<0$ for every $i\in\mathbb{N}_0$.

Therefore, both sequences are bounded, and since by Lemma 3.2 they are monotonic, then they are convergent. □

Proposition 3.7: If the functions f_1 and f_2 in (3) satisfy the strict version of inequalities (12) and (13) given by

$$(f_1(\upsilon,\gamma_1)-f_1(\upsilon,\gamma_2))(\gamma_1-\gamma_2)<0, \tag{18}$$
$$(f_2(\upsilon,\gamma_1)-f_2(\upsilon,\gamma_2))(\gamma_1-\gamma_2)>0, \tag{19}$$

for every $\gamma_1\neq\gamma_2$ and $\upsilon\in\mathbb{R}$, then there exist a unique pair $\gamma_*,\zeta_*\in\mathbb{R}$ such that for every $\gamma_0\in\mathbb{R}$ the sequences generated by (10) and (11) satisfy $(\gamma_n)_{n\in\mathbb{N}_0}\to\gamma_*$ and $(\zeta_n)_{n\in\mathbb{N}_0}\to\zeta_*$ where $\zeta_* = \mathcal{Y}_{u_{p+}}(\upsilon_{\max},\gamma_*)$.

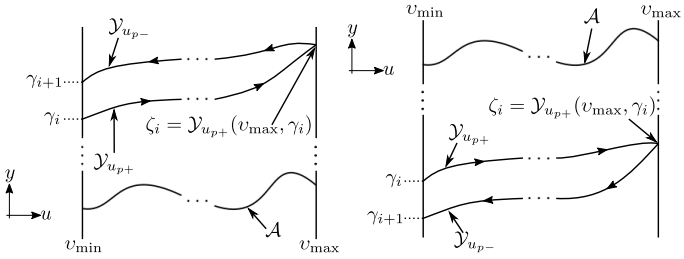

(a) Strictly increasing $(\gamma_n)_{n\in\mathbb{N}_0}$. (b) Strictly decreasing $(\gamma_n)_{n\in\mathbb{N}_0}$.

Figure 2: Contradiction cases in proof of Proposition 3.5 for strictly monotonic unbounded sequence $(\gamma_n)_{n\in\mathbb{N}_0}$.

PROOF: We proceed by contradiction, assuming that the sequences $(\gamma_n)_{n\in\mathbb{N}_0}$ and $(\zeta_n)_{n\in\mathbb{N}_0}$ approach different values if we used different initial values. For this, assume there exists $\bar\gamma\neq\gamma_*$ and two initial values $\gamma_i\neq\gamma_j$ such that $\lim_{i\to\infty}(\gamma_i-\gamma_*)=0$ and $\lim_{j\to\infty}(\gamma_j-\bar\gamma)=0$. We can subtract both limits and use (16) to obtain

$$\begin{aligned}
0 &= \lim_{i\to\infty}(\gamma_i-\gamma_*) - \lim_{j\to\infty}(\gamma_j-\bar\gamma)\\
&= \int_{\upsilon_{\min}}^{\upsilon_{\max}} \left\{ f_1\left(\nu,\mathcal{Y}_{u_{p+}}(\nu,\gamma_*)\right) - f_2\left(\nu,\mathcal{Y}_{u_{p-}}(\nu,\zeta_*)\right)\right\}\mathrm{d}\nu\\
&\quad - \int_{\upsilon_{\min}}^{\upsilon_{\max}} \left\{ f_1\left(\nu,\mathcal{Y}_{u_{p+}}(\nu,\bar\gamma)\right) - f_2\left(\nu,\mathcal{Y}_{u_{p-}}(\nu,\bar\zeta)\right)\right\}\mathrm{d}\nu\\
&= \int_{\upsilon_{\min}}^{\upsilon_{\max}} \left\{ f_1\left(\nu,\mathcal{Y}_{u_{p+}}(\nu,\gamma_*)\right) - f_1\left(\nu,\mathcal{Y}_{u_{p+}}(\nu,\bar\gamma)\right)\right\}\mathrm{d}\nu\\
&\quad - \int_{\upsilon_{\min}}^{\upsilon_{\max}} \left\{ f_2\left(\nu,\mathcal{Y}_{u_{p-}}(\nu,\zeta_*)\right) - f_2\left(\nu,\mathcal{Y}_{u_{p-}}(\nu,\bar\zeta)\right)\right\}\mathrm{d}\nu
\end{aligned} \tag{20}$$

where $\zeta_* = \mathcal{Y}_{u_{p+}}(\upsilon_{\max},\gamma_*)$ and $\bar\zeta = \mathcal{Y}_{u_{p+}}(\upsilon_{\max},\bar\gamma)$. Then, by (18) and (19) and Lemma 3.1, the right term of the last expression is positive (resp. negative) when $\gamma_*<\bar\gamma$ and $\zeta*<\bar\zeta$ (resp. $\gamma_*>\bar\gamma$ and $\zeta*>\bar\zeta$), which is a contradiction. □

Finally, to complement the previous two propositions, we also establish conditions such that the sequences $(\gamma_n)_{n\in\mathbb{N}_0}$ and $(\zeta_n)_{n\in\mathbb{N}_0}$ generated by (10) and (11) are divergent. The conditions are presented in the proposition below.

Proposition 3.8: If the functions f_1 and f_2 in the Duhem model (3) satisfy the reversed inequalities to (18) and (19), which are given by

$$(f_1(\upsilon,\gamma_1)-f_1(\upsilon,\gamma_2))(\gamma_1-\gamma_2)>0, \tag{21}$$
$$(f_2(\upsilon,\gamma_1)-f_2(\upsilon,\gamma_2))(\gamma_1-\gamma_2)<0, \tag{22}$$

for every $\gamma_1\neq\gamma_2$ and $\upsilon\in\mathbb{R}$, then for every $\gamma_0\in\mathbb{R}$ such that

$$\int_{\upsilon_{\min}}^{\upsilon_{\max}} \left\{ f_1\left(\nu,\mathcal{Y}_{u_{p+}}(\upsilon,\gamma_0)\right) - f_2\left(\nu,\mathcal{Y}_{u_{p-}}(\upsilon,\zeta_0)\right)\right\}\mathrm{d}\nu \neq 0, \tag{23}$$

with $\zeta_0 = \mathcal{Y}_{u_{p+}}(\upsilon_{\max},\gamma_0)$, the sequences $(\zeta_n)_{n\in\mathbb{N}_0}$ and $(\gamma_n)_{n\in\mathbb{N}_0}$ generated by (10) and (11) are divergent.

PROOF: Note that when (23) does not holds, then from (16) we have $\gamma_1-\gamma_0=0$ and by Lemma 3.3 all the terms of both sequences are equal.

Therefore, let (23) hold. We prove the case when both sequences are increasing and unbounded. Assume that $\gamma_i > \gamma_{i-1}$. Replacing $\upsilon = \upsilon_{\max}$ into (14), we can obtain

$$\begin{aligned}&\zeta_i - \zeta_{i-1}\\ &= \int_{\upsilon_{\min}}^{\upsilon_{\max}} \left\{ f_1\left(\nu, \mathcal{Y}_{u_{p+}}(\nu,\gamma_i)\right) - f_1\left(\nu, \mathcal{Y}_{u_{p+}}(\nu,\gamma_{i-1})\right) \right\} \mathrm{d}\nu \\ &\qquad + \gamma_i - \gamma_{i-1},\end{aligned}$$

where the integral is positive following (21) and Lemma 3.1. Therefore, we obtain $\zeta_i - \zeta_{i-1} > \gamma_i - \gamma_{i-1} > 0$. In a similar form, replacing $\upsilon = \upsilon_{\min}$ into (15), we have

$$\begin{aligned}&\gamma_{i+1} - \gamma_i\\ &= -\int_{\upsilon_{\min}}^{\upsilon_{\max}} \left\{ f_2\left(\nu, \mathcal{Y}_{u_{p-}}(\nu,\zeta_i)\right) - f_2\left(\nu, \mathcal{Y}_{u_{p-}}(\nu,\zeta_{i-1})\right) \right\} \mathrm{d}\nu \\ &\qquad + \zeta_i - \zeta_{i-1}.\end{aligned}$$

where the integral is negative following from (22) and Lemma 3.1. Thus we obtain $\gamma_{i+1} - \gamma_i > \zeta_i - \zeta_{i-1}$. Combining both inequalities, we obtain $\gamma_{i+1} - \gamma_i > \gamma_i - \gamma_{i-1} > 0$, and consequently the sequence $(\gamma_n)_{n\in\mathbb{N}_0}$ is increasing and unbounded. Moreover, by Lemma 3.4 $(\zeta_n)_{n\in\mathbb{N}_0}$ is also increasing and unbounded.

Similar argumentation holds for the case when both sequences are decreasing and unbounded by reversing all inequalities above. □

C. Case Example: the Bouc-Wen model

We use now the propositions presented in this section to study a particular case of the Bouc-Wen hysteresis model [32]–[34]. The Bouc-Wen model is commonly used to describe relations between displacement and restoring force as input and output in piezoactuated mechanical systems and it is defined by

$$\dot{y}(t) = \alpha\dot{u}(t) - \beta\,|y(t)|^n\,\dot{u}(t) - \zeta y(t)\,|y(t)|^{n-1}\,|\dot{u}(t)|\,,$$

where $\alpha, \beta, \zeta \in \mathbb{R}$ are model parameters. The equation above can be also written as a Duhem model of the form (3) whose vector field functions f_1 and f_2 are defined by

$$\begin{aligned}f_1(\upsilon,\gamma) &:= \alpha - \beta\,|\gamma|^n - \zeta\gamma|\gamma|^{n-1},\\ f_2(\upsilon,\gamma) &:= \alpha - \beta\,|\gamma|^n + \zeta\gamma|\gamma|^{n-1}.\end{aligned}$$

Using these f_1 and f_2 into (12) and (13) of Proposition 3.5 we have

$$\begin{aligned}&[(\beta + \zeta\,\mathrm{sign}(\gamma_1))\,|\gamma_1|^n - (\beta + \zeta\,\mathrm{sign}(\gamma_2))\,|\gamma_2|^n]\,(\gamma_1 - \gamma_2) \geq 0,\\ &[(\beta - \zeta\,\mathrm{sign}(\gamma_1))\,|\gamma_1|^n - (\beta - \zeta\,\mathrm{sign}(\gamma_2))\,|\gamma_2|^n]\,(\gamma_1 - \gamma_2) \leq 0.\end{aligned}$$

Assuming without loss of generality that $\gamma_1 > \gamma_2$, we obtain

$$[(\beta + \zeta\,\mathrm{sign}(\gamma_1))\,|\gamma_1|^n - (\beta + \zeta\,\mathrm{sign}(\gamma_2))\,|\gamma_2|^n] \geq 0, \quad (24)$$
$$[(\beta - \zeta\,\mathrm{sign}(\gamma_1))\,|\gamma_1|^n - (\beta - \zeta\,\mathrm{sign}(\gamma_2))\,|\gamma_2|^n] \leq 0. \quad (25)$$

Note now that when $\gamma_1 > \gamma_2 \geq 0$ or $0 \geq \gamma_1 > \gamma_2$, we can reduce (24) and (25) to

$$\begin{aligned}(\beta + \zeta)\,(|\gamma_1|^n - |\gamma_2|^n) \geq 0,\\ (\beta - \zeta)\,(|\gamma_1|^n - |\gamma_2|^n) \leq 0,\end{aligned}$$

respectively, which are trivially satisfied when

$$\beta + \zeta \geq 0, \quad (26)$$
$$\beta - \zeta \leq 0. \quad (27)$$

Moreover, when $\gamma_1 > 0 > \gamma_2$ we have

$$\begin{aligned}\beta\,(|\gamma_1|^n - |\gamma_2|^n) + \zeta\,(|\gamma_1|^n + |\gamma_2|^n) \geq 0\\ \beta\,(|\gamma_1|^n - |\gamma_2|^n) - \zeta\,(|\gamma_1|^n + |\gamma_2|^n) \leq 0\end{aligned}$$

which are also satisfied for (26) and (27).

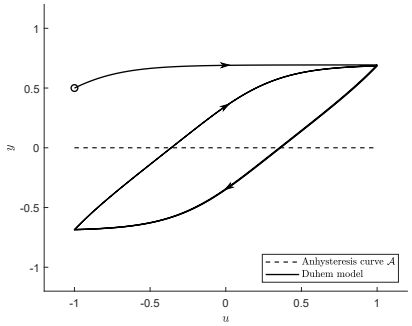

Figure 3: Hysteresis loop obtained from a Bouc-Wen hysteresis operator whose parameters $\alpha = 1$, $\beta = 2$, $\zeta = 1$ satisfy the convergence conditions in (26) and (27) when a periodic input whose minimum and maximum are $\upsilon_{\min} = -1$ and $\upsilon_{\max} = 1$ is applied. The initial point $(u(0), y(0)) = (\upsilon_{\min}, y_0)$ is marked by a circle.

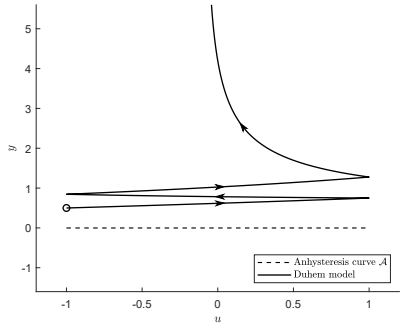

Figure 4: Divergent input-output phase plot obtained from a Bouc-Wen hysteresis operator whose parameters $\alpha = 0.1$, $\beta = 0.1$, $\zeta = -0.2$ satisfy the divergence conditions in (28) and (29) when a periodic input whose minimum and maximum are $\upsilon_{\min} = -1$ and $\upsilon_{\max} = 1$ is applied. The initial point $(u(0), y(0)) = (\upsilon_{\min}, y_0)$ is marked by a circle.

Therefore, the sequences defined by (10) and (11) are convergent for every initial value $\gamma_0 \in \mathbb{R}$, or equivalently, the input-output phase plot of the Bouc-Wen model will converge to a periodic orbit from every initial point when conditions in (26) and (27) are satisfied. In fact, it can be checked that these conditions are equivalent to the ones presented in [32, Table 1] corresponding to BIBO stable Bouc-Wen models of

class I, III and V. As an illustrative example, the input-output phase plot of a Bouc-Wen model whose parameters satisfy the convergence conditions in (26) and (27) with $\alpha = 1$, $\beta = 1$ and $\zeta = 2$ is shown in Fig. 3.

Conversely, based on Proposition 3.8, when we have the reversed inequalities

$$\beta + \zeta < 0, \tag{28}$$
$$\beta - \zeta > 0. \tag{29}$$

then the sequences defined by (10) and (11) will diverge which means that the input-output phase plot Bouc-Wen model will not exhibit a hysteresis loop. An example of this case is illustrated in Fig. 4 with the divergent input-output phase plot of a Bouc-Wen model whose parameters are $\alpha = 0.1$, $\beta = 0.1$ and $\zeta = -0.2$.

IV. THE DUHEM BUTTERFLY MODEL

In this section, we introduce a special class of Duhem operators which we call the Duhem butterfly operators. This operator is characterized by its capability in producing complex periodic hysteresis loops with self-intersections. In this class of operators both functions f_1 and f_2 in (3) can assume positive and negative values as long as they satisfy the conditions (18) and (19), respectively, to guarantee the existence of a unique periodic solution.

We assume now that the implicit functions $\upsilon \mapsto \{\gamma \mid f_1(\upsilon,\gamma) = 0\}$ and $\upsilon \mapsto \{\gamma \mid f_2(\upsilon,\gamma) = 0\}$ admit explicit solutions

$$\gamma = c_1(\upsilon) \qquad \text{and} \qquad \gamma = c_2(\upsilon), \tag{30}$$

respectively, with $c_1, c_2 \in AC(\mathbb{R},\mathbb{R})$ such that $f_1(\upsilon, c_1(\upsilon)) = 0$ and $f_2(\upsilon, c_2(\upsilon)) = 0$ for every $\upsilon \in \mathbb{R}$. In other words, the curves described by c_1 and c_2 are the zero level set of the functions f_1 and f_2, respectively. Note that by conditions (18) and (19), each of the curves c_1 and c_2 split the input-output plane $u - y$ into two regions such that

$$\begin{aligned}
&f_1(\upsilon,\gamma) < 0 \text{ whenever } \gamma > c_1(\upsilon);\\
&f_1(\upsilon,\gamma) > 0 \text{ whenever } \gamma < c_1(\upsilon);\\
&f_2(\upsilon,\gamma) > 0 \text{ whenever } \gamma > c_2(\upsilon); \text{and}\\
&f_2(\upsilon,\gamma) < 0 \text{ whenever } \gamma > c_2(\upsilon).
\end{aligned}$$

In the following, we will prove that when the functions f_1 and f_2, and the zero-level set functions c_1 and c_2 satisfy some mild assumptions, there is a periodic hysteresis loop with a self-intersection which gives the existence of a butterfly hysteresis loop. Prior to this, we need to introduce the following notations. Let $u_+, u_- \in AC(\mathbb{R}_+,\mathbb{R})$ be inputs which are monotonically increasing and decreasing, respectively, and radially unbounded, i.e. $u_+(t) \to \infty$ and $u_-(t) \to -\infty$ as $t \to \infty$, respectively. Similar to (8) and (9), we define the solutions of the Duhem model (3) parameterized by the instantaneous value of the inputs u_+ and u_- by y_{u_+} and y_{u_-}, respectively. The next lemma shows, under mild assumptions on the functions c_1 and c_2, the positive invariance of the region below the curves c_1 and c_2 with respect to the solutions of y_{u_+} and y_{u_-}, respectively.

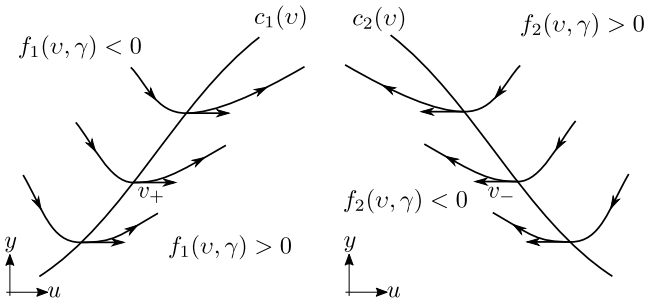

(a) With an increasing input u_+.

(b) With a decreasing input u_-.

Figure 5: Invariance of the solutions for an increasing and decreasing input respect to the parameterizations $c_1(\upsilon)$ and $c_2(\upsilon)$ of the level sets $f_1(\upsilon,\gamma) = 0$ and $f_2(\upsilon,\gamma) = 0$, respectively.

Lemma 4.1: If $0 \le \frac{dc_1(\upsilon)}{d\upsilon} \le L_1$ for all $\upsilon \ge u_+(0)$ then for all $\gamma_0 \le c_1(u_+(0))$, $y_{u_+}(\upsilon,\gamma_0) \le c_1(\upsilon)$ for all $\upsilon \ge u_+(0)$.

Analogously, if $-L_2 \le \frac{dc_2(\upsilon)}{d\upsilon} \le 0$ for all $\upsilon \le u_-(0)$ then for all $\gamma_0 \le c_2(u_-(0))$, $y_{u_-}(\upsilon,\gamma_0) \le c_2(\upsilon)$ for all $\upsilon \le \upsilon_0$.

PROOF: We prove now the first claim of the lemma. Let us define the domain under the curve c_1 as follows

$$\mathcal{C}_{1+} := \left\{(\upsilon,\gamma) \in \mathbb{R}^2 \mid \gamma \le c_1(\upsilon)\right\}. \tag{31}$$

It can be checked that $\mathcal{C}_{1+}$ is positively invariant with respect to the solutions of Duhem model (3) with monotonically increasing input u_+ and with initial conditions in $\mathcal{C}_{1+}$. Indeed, for every point $x \in \mathcal{C}_{1+}$ we can construct the tangent cone to this set as defined in [35, Def. 3.1], which is given by

$$\mathcal{T}_{\mathcal{C}_{1+}}(x) = \left\{ z \in \mathbb{R}^2 \colon \liminf_{h \to 0} \frac{\operatorname{dist}(x + hz, \mathcal{C}_{1+})}{h} = 0 \right\},$$

where we take $\operatorname{dist}(\cdot)$ to be the Euclidian distance from x to the closest point $y \in \mathcal{C}_{1+}$. Let $v_+(\upsilon_0) \in \mathbb{R}^2$ be the tangent vector to the solution y_{u_+} which is given by

$$\begin{aligned}
v_+(\upsilon_0) &= \left(1, \frac{\mathrm{d}}{\mathrm{d}\upsilon}\bigg|_{\upsilon=\upsilon_0} y_{u_+}\big(\upsilon, c_1(\upsilon_0)\big)\right)\\
&= \Big(1, f_1\big(\upsilon_0, c_1(\upsilon_0)\big)\Big).
\end{aligned}$$

Now, we show that $v_+(\upsilon_0) \in \mathcal{T}_{\mathcal{C}_{1+}}(x_1)$ with $x_1 = (\upsilon_0, c_1(\upsilon_0)) \in \mathcal{C}_{1+}$ for every $\upsilon_0 \in \mathbb{R}$ so that the solutions of y_{u_+} do not escape $\mathcal{C}_{1+}$ on the boundary (see Fig. 5a). In other words, we show that the tangent vector to the solution y_{u_+} belongs to the tangent cone of the set $\mathcal{C}_{1+}$ at every point of the boundary. For this let us consider a point $w = (\upsilon_0 + h, c_1(\upsilon_0))$ and note that since $c_1(\upsilon)$ is monotonically increasing we have $w \in \mathcal{C}_{1+}$ for every $h > 0$. Then we can check

$$\begin{aligned}
&\liminf_{h \to 0^+} \frac{\big\|\big(x_1 + h v_+(\upsilon_0)\big) - w\big\|}{h}\\
&\quad = \liminf_{h \to 0^+} \frac{h\big|f_1\big(\upsilon_0, c_1(\upsilon_0)\big)\big|}{h} = \big|f_1\big(\upsilon_0, c_1(\upsilon_0)\big)\big| = 0,
\end{aligned}$$

which proves that $\nu_+(\upsilon_0) \in \mathcal{T}_{\mathcal{C}_{2-}}(x_1)$. Consequently, following from Nagumo's theorem [35, Th. 3.1] the set $\mathcal{C}_{1+}$ is positively invariant and $\mathcal{Y}_{u_+}(\upsilon,\gamma_0) \leq c_1(\upsilon)$ for every $\upsilon \geq \upsilon_0$.

For proving the second claim of the lemma, we consider the set

$$\mathcal{C}_{2-} := \left\{(\upsilon,\gamma) \in \mathbb{R}^2 \mid \gamma \leq c_2(\upsilon)\right\}, \tag{32}$$

which consists of all the points below the curve parameterized by $\gamma = c_2(\upsilon)$. We let $\nu_-(\upsilon_0) \in \mathbb{R}^2$ be the tangent vector to the solution $\mathcal{Y}_{u_-}$ given by

$$\begin{aligned}\nu_-(\upsilon_0) &= \left(-1, \frac{\mathrm{d}}{\mathrm{d}\upsilon}\bigg|_{u=\upsilon_0} \mathcal{Y}_{u_-}\big(\upsilon, c_2(\upsilon_0)\big)\right) \\ &= \Big(-1, f_2\big(\upsilon_0, c_2(\upsilon_0)\big)\Big).\end{aligned}$$

In this case, we show that the tangent vector $\nu_-(\upsilon_0)$ to the solution $\mathcal{Y}_{u_-}$ belongs to the tangent cone of the set $\mathcal{C}_{2-}$ at every point of the boundary (see Fig. 5b). We consider in this case a point $w = (\upsilon_0 - h, c_2(\upsilon_0))$ and note that since $c_2(\upsilon)$ is monotonically decreasing we have $w \in \mathcal{C}_{2-}$ for every $h > 0$. Then we can check analogously that

$$\begin{aligned}&\liminf_{h\to 0^+} \frac{\|\big(x_2 + h\nu_-(\upsilon_0)\big) - w\|}{h} \\ &\quad = \liminf_{h\to 0^+} \frac{h|f_2\big(\upsilon_0, c_2(\upsilon_0)\big|}{h} = |f_2\big(\upsilon_0, c_2(\upsilon_0)\big)| = 0,\end{aligned}$$

which proves that $\nu_-(\upsilon_0) \in \mathcal{T}_{\mathcal{C}_{2-}}(x_2)$ and following again from Nagumo's theorem the set $\mathcal{C}_{2-}$ is positively invariant and $\mathcal{Y}_{u_-}(\upsilon,\gamma_0) \leq c_2(\upsilon)$ for every $\upsilon \leq \upsilon_0$. □

We remark that Lemma 4.1 proves invariance of the solutions only for the case when the slopes of the level set functions c_1 and c_2 in (30) are positive and negative, respectively. Nevertheless, it is also possible to prove invariance for the opposite case corresponding to the level set functions c_1 and c_2 having negative and positive slopes, respectively. In this opposite case, the invariant set for $\mathcal{Y}_{u_+}$ and $\mathcal{Y}_{u_-}$ correspond to the closure of the complement of $\mathcal{C}_{1+}$ in (31) and $\mathcal{C}_{2-}$ in (32), respectively.

In the next lemma we prove that under mild assumptions regarding the monotonicity in the first argument of the functions f_1 and f_2, the extended solutions $\mathcal{Y}_{u_+}$ and $\mathcal{Y}_{u_-}$ in the reverse direction (when the input signal u_+ and u_- as defined before Lemma 4.1 are extended from $\mathbb{R}_+$ to the whole real $\mathbb{R}$) intersect with the zero level set curve c_2 and c_1, respectively.

Lemma 4.2: Assume that the hypotheses in Lemma 4.1 hold. Suppose that f_1 satisfy

$$\big(f_1(\upsilon_1,\gamma) - f_1(\upsilon_2,\gamma)\big)(\upsilon_1 - \upsilon_2) < 0, \tag{33}$$

for every $\upsilon_1, \upsilon_2, \gamma \in \mathbb{R}$ and let $\upsilon_a, \gamma_a \in \mathbb{R}$ be such that $\gamma_a = c_1(\upsilon_a) < c_2(\upsilon_a)$. Then there exists $\upsilon_b < \upsilon_a$ such that $\mathcal{Y}_{u_+}(\upsilon_b,\gamma_a) = c_2(\upsilon_b)$.

Analogously, suppose that f_2 satisfy

$$\big(f_2(\upsilon_1,\gamma) - f_2(\upsilon_2,\gamma)\big)(\upsilon_1 - \upsilon_2) > 0, \tag{34}$$

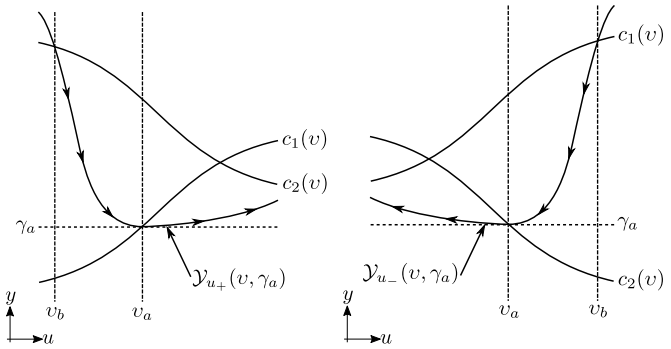

(a) Intersection of the level set curve $\gamma = c_1(\upsilon)$ and the solution $\mathcal{Y}_{u_-}(\upsilon,\gamma_a)$.

(b) Intersection of the level set curve $\gamma = c_2(\upsilon)$ and the solution $\mathcal{Y}_{u_+}(\upsilon,\gamma_a)$.

Figure 6: Intersection of the solutions for an increasing and decreasing input with the parameterizations $c_1(\upsilon)$ and $c_2(\upsilon)$ of the level sets $f_1(\upsilon,\gamma) = 0$ and $f_2(\upsilon,\gamma) = 0$, respectively.

for every $\upsilon_1, \upsilon_2, \gamma \in \mathbb{R}$ and let $\upsilon_a, \gamma_a \in \mathbb{R}$ be such that $\gamma_a = c_1(\upsilon_a) > c_2(\upsilon_a)$. Then there exists $\upsilon_b > \upsilon_a$ such that $\mathcal{Y}_{u_-}(\upsilon_b,\gamma_a) = c_1(\upsilon_b)$.

PROOF: Let us firstly prove the existence of a point υ_b where the curve $\mathcal{Y}_{u+}(\cdot,\gamma_a)$ intersects with c_2 at υ_b. By extending u_+ from $\mathbb{R}_+$ to $\mathbb{R}$ while still satisfying the monotonicity and radial unbounded assumption of u_+ (e.g., $\lim_{t\to-\infty} u_+(t) = -\infty$ and $\lim_{t\to+\infty} u_+(t) = \infty$), the solution $\mathcal{Y}_{u_+}(\upsilon,\gamma_a)$ can be extended in the negative direction (i.e. $\upsilon < \upsilon_a$) and the equation

$$\begin{aligned}\mathcal{Y}_{u_+}(\upsilon,\gamma_a) = &\int_{\upsilon_a}^{\upsilon} f_1\left(\nu, \mathcal{Y}_{u_+}(\nu,\gamma_a)\right)\,\mathrm{d}\nu + \gamma_a \\ &= -\int_{\upsilon}^{\upsilon_a} f_1\left(\nu, \mathcal{Y}_{u_+}(\nu,\gamma_a)\right)\,\mathrm{d}\nu + \gamma_a,\end{aligned}$$

is still valid (see Fig. 6a). Moreover, since $f_1(\upsilon,\gamma) < 0$ whenever $\gamma > c_1(\upsilon)$ we have that

$$\mathcal{Y}_{u_+}(\upsilon,\gamma_a) = \left|\int_{\upsilon}^{\upsilon_a} f_1\left(\nu, \mathcal{Y}_{u_+}(\nu,\gamma_a)\right)\,\mathrm{d}\nu\right| + \gamma_a,$$

for every $\upsilon < \upsilon_a$, which means that the extension of the solution $\mathcal{Y}_{u_+}(\upsilon,\gamma_a)$ in the negative direction remains above the curve parameterized by $\gamma = c_1(\upsilon)$. By the assumption (33) and using the bound L_2 of $\frac{dc_2(\upsilon)}{d\upsilon}$ as in the hypotheses of Lemma 4.1, we have that there exists $\upsilon_{L_2} \leq \upsilon_a$ such that for every $\upsilon < \upsilon_{L_2}$ we have

$$f_1\left(\upsilon, \mathcal{Y}_{u_+}(\upsilon,\gamma_a)\right) < f_1\left(\upsilon_{L_2}, \mathcal{Y}_{u_+}(\upsilon_{L_2},\gamma_a)\right) = -L_2.$$

Since we have that

$$\begin{aligned}c_2(\upsilon) &= \int_{\upsilon_a}^{\upsilon} \frac{\mathrm{d}c_2}{\mathrm{d}\upsilon}\mathrm{d}\upsilon + c_2(\upsilon_a) \\ &= -\int_{\upsilon}^{\upsilon_a} \frac{\mathrm{d}c_2}{\mathrm{d}\upsilon}\mathrm{d}\upsilon + c_2(\upsilon_a) \leq L_2(\upsilon_a - \upsilon) + c_2(\upsilon_a),\end{aligned}$$

the solution $\mathcal{Y}_{u_+}(\upsilon,\gamma_a)$ and the curve parameterized by $\gamma = c_2(\upsilon)$ intersect each other at some $\upsilon_b < \upsilon_{L_2}$. Indeed, this can be observed from the fact that

$$\begin{aligned}\mathcal{Y}_{u_+}(\upsilon,\gamma_a) - c_2(\upsilon) &= \gamma_a - c_2(\upsilon_a) \\ &\quad + \int_{\upsilon_a}^{\upsilon} \left\{ f_1\left(\upsilon, \mathcal{Y}_{u_+}(\upsilon,\gamma_a)\right) - \frac{\mathrm{d}c_2}{\mathrm{d}\upsilon} \right\} \mathrm{d}\upsilon \\ &= \underbrace{\int_{\upsilon_a}^{\upsilon_{L_2}} \left\{ f_1\left(\upsilon, \mathcal{Y}_{u_+}(\upsilon,\gamma_a)\right) - \frac{\mathrm{d}c_2}{\mathrm{d}\upsilon} \right\} \mathrm{d}\upsilon}_{<0} \\ &\quad + \underbrace{\int_{\upsilon_{L_2}}^{\upsilon} \left\{ f_1\left(\upsilon, \mathcal{Y}_{u_+}(\upsilon,\gamma_a)\right) - \frac{\mathrm{d}c_2}{\mathrm{d}\upsilon}, \right\} \mathrm{d}\upsilon}_{\geq 0}\end{aligned}$$

where the last term grows radially unbounded for $\upsilon < \upsilon_{L_2}$.

We can prove analogously the second claim of the lemma as illustrated in Fig. 6b. Similar as before, the solution $\mathcal{Y}_{u_-}(\upsilon,\gamma_a)$ can be extended in the positive direction (i.e. $\upsilon > \upsilon_a$) when u_- is extended from $\mathbb{R}_+$ to $\mathbb{R}$ satisfying the monotonicity and radial unbounded assumption of u_-. In this case,

$$\mathcal{Y}_{u_-}(\upsilon,\gamma_a) = \int_{\upsilon_a}^{\upsilon} f_2\left(\nu, \mathcal{Y}_{u_-}(\nu,\gamma_a)\right)\ \mathrm{d}\nu + \gamma_a$$

and since $f_2(\upsilon,\gamma) > 0$ whenever $\gamma > c_2(\upsilon)$, we have that

$$\mathcal{Y}_{u_-}(\upsilon,\gamma_a) = \left| \int_{\upsilon}^{\upsilon_a} f_2\left(\nu, \mathcal{Y}_{u_-}(\nu,\gamma_a)\right)\ \mathrm{d}\nu \right| + \gamma_a,$$

for every $\upsilon > \upsilon_a$, which means that the extension of the solution $\mathcal{Y}_{u_-}(\upsilon,\gamma_a)$ in the positive direction remains above the curve parameterized by $\gamma = c_2(\upsilon)$. In this case, using (34) and the bound L_1 of $\frac{dc_1(\upsilon)}{d\upsilon}$, we have that there exists $\upsilon_{L_1} \geq \upsilon_a$ such that for every $\upsilon > \upsilon_{L_1}$ we have

$$f_2\left(\upsilon, \mathcal{Y}_{u_-}(\upsilon,\gamma_a)\right) > f_2\left(\upsilon_{L_1}, \mathcal{Y}_{u_-}(\upsilon_{L_1},\gamma_a)\right) = L_1.$$

Since we have that

$$c_1(\upsilon) = \int_{\upsilon_a}^{\upsilon} \frac{\mathrm{d}c_1}{\mathrm{d}\upsilon}\mathrm{d}\upsilon + c_1(\upsilon_a) \leq L_1(\upsilon - \upsilon_a) + c_1(\upsilon_a),$$

the solution $\mathcal{Y}_{u_-}(\upsilon,\gamma_a)$ and the curve parameterized by $\gamma = c_1(\upsilon)$ intersect each other at some $\upsilon_b > \upsilon_{L_1}$. It follows from the fact that

$$\begin{aligned}\mathcal{Y}_{u_-}(\upsilon,\gamma_a) - c_1(\upsilon) &= \gamma_a - c_1(\upsilon_a) \\ &\quad + \int_{\upsilon_a}^{\upsilon} \left\{ f_2\left(\upsilon, \mathcal{Y}_{u_-}(\upsilon,\gamma_a)\right) - \frac{\mathrm{d}c_1}{\mathrm{d}\upsilon} \right\} \mathrm{d}\upsilon \\ &= \underbrace{\int_{\upsilon_a}^{\upsilon_{L_1}} \left\{ f_2\left(\upsilon, \mathcal{Y}_{u_-}(\upsilon,\gamma_a)\right) - \frac{\mathrm{d}c_1}{\mathrm{d}\upsilon} \right\} \mathrm{d}\upsilon}_{<0} \\ &\quad + \underbrace{\int_{\upsilon_{L_1}}^{\upsilon} \left\{ f_2\left(\upsilon, \mathcal{Y}_{u_-}(\upsilon,\gamma_a)\right) - \frac{\mathrm{d}c_1}{\mathrm{d}\upsilon}, \right\} \mathrm{d}\upsilon}_{\geq 0}\end{aligned}$$

where the last term grows radially unbounded for $\upsilon > \upsilon_{L_1}$. □

As with Lemma 4.1, we also remark that Lemma 4.2 proves that the extension of the solutions in the negative direction of their corresponding input intersect with the zero level set functions c_1 and c_2 only for the case when their slopes are positive and negative, respectively. However, vis-a-vis arguments can prove the opposite case when the extended solutions in the negative direction of their corresponding input intersect with the level set functions c_1 and c_2 have negative and positive slopes, respectively.

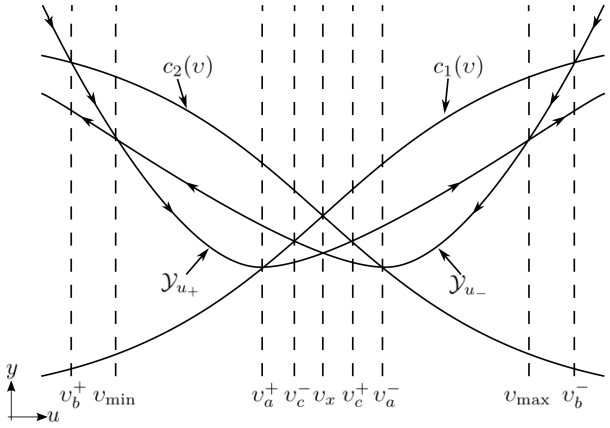

Figure 7: Construction of butterfly loop from the intersections of two solutions $\mathcal{Y}_{u_+}$ and $\mathcal{Y}_{u_-}$.

In the following proposition we present the main result of this section, where we prove constructively the existence of outputs $\mathcal{Y}_{u_+}$ and $\mathcal{Y}_{u_-}$ with intersections.

Proposition 4.3: Assume that the hypotheses in Lemma 4.2 are satisfied (which include those in Lemmas 4.1). Let $\upsilon_f \in \mathbb{R}$ be such that $c_1(\upsilon_f) = c_2(\upsilon_f)$. Then for every $\upsilon_{a_+} < \upsilon_f$ there exist $\upsilon_{\min}, \upsilon_x, \upsilon_{a_-}, \upsilon_{\max} \in \mathbb{R}$ such that $\upsilon_{\min} < \upsilon_{a_+} < \upsilon_x < \upsilon_{a_-} < \upsilon_{\max}$ and

$$\begin{aligned}\mathcal{Y}_{u_+}(\upsilon_{\min}, c_1(\upsilon_{a_+})) &= \mathcal{Y}_{u_-}(\upsilon_{\min}, c_2(\upsilon_{a_-})) \\ \mathcal{Y}_{u_+}(\upsilon_x, c_1(\upsilon_{a_+})) &= \mathcal{Y}_{u_-}(\upsilon_x, c_2(\upsilon_{a_-})) \\ \mathcal{Y}_{u_+}(\upsilon_{\max}, c_1(\upsilon_{a_+})) &= \mathcal{Y}_{u_-}(\upsilon_{\max}, c_2(\upsilon_{a_-})).\end{aligned}$$

In other words, the solutions $\mathcal{Y}_{u_+}(\cdot, c_1(\upsilon_{a_+}))$ and $\mathcal{Y}_{u_-}(\cdot, c_2(\upsilon_{a_-}))$ which intersect c_1 and c_2 at υ_{a_+} and υ_{a_-}, respectively, intersect also each other at υ_x, $\upsilon_{\min}$ and $\upsilon_{\max}$.

PROOF: For a better understanding of the constructive proof of this proposition we refer the reader to Fig. 7.
Consider the solution $\mathcal{Y}_{u_+}(\upsilon, c_1(\upsilon_{a_+}))$. By Lemma 4.2 there exists $\upsilon_{b_+} < \upsilon_{a_+}$ where this solution intersects the curve c_2 i.e.

$$\mathcal{Y}_{u_+}(\upsilon_{b_+}, c_1(\upsilon_{a_+})) = c_2(\upsilon_{b_+}).$$

Additionally, by Lemma 4.1 we have that the solution $\mathcal{Y}_{u_+}$ remains below the curve c_1 for every $\upsilon > \upsilon_{a_+}$ but always increasing as υ increases since $f_1(\upsilon,\gamma) > 0$ when $\gamma < c_1(\upsilon)$. Therefore, since $\frac{dc_2}{d\upsilon} \leq 0$, then the solution $\mathcal{Y}_{u_+}$ must also intersect the curve c_2 at some $\upsilon_{c_+} > \upsilon_{a_+}$ i.e.

$$\mathcal{Y}_{u_+}(\upsilon_{c_+}, c_1(\upsilon_{a_+})) = c_2(\upsilon_{c_+}).$$

Let us define now $\upsilon_{a_-} = \upsilon_{c_+} + \varepsilon$ with $\varepsilon > 0$ being arbitrarily small and consider the solution $\gamma_{u_-}(\upsilon, c_2(\upsilon_{a_-}))$. As in the previous case, by Lemma 4.2 there exists $\upsilon_{b_-} > \upsilon_{a_-}$ where this solution intersects the curve c_1 i.e.

$$\gamma_{u_-}(\upsilon_{b_-}, c_2(\upsilon_{a_-})) = c_1(\upsilon_{b_-}).$$

We can also note that by Lemma 4.1 the solution γ_{u_-} remains below the curve c_2 but always increasing as υ decreases given that $f_2(\upsilon,\gamma) > 0$ for every $\upsilon < \upsilon_{a_-}$. Consequently, since $\frac{dc_1}{d\upsilon} \geq 0$, then the solution γ_{u_-} must also intersect the curve c_1 at some $\upsilon_{c_-} < \upsilon_{a_-}$ i.e.

$$\gamma_{u_-}(\upsilon_{c_-}, c_2(\upsilon_{a_-})) = c_1(\upsilon_{c_-}).$$

If the value υ_{c_-} satisfies $\upsilon_{c_-} > \upsilon_{a_+}$ it is clear that the solution γ_{u_-} intersects with γ_{u_+} at some υ_x such that $\upsilon_{a_+} < \upsilon_x < \upsilon_{a_-}$. In the opposite case that $\upsilon_{c_-} < \upsilon_{a_+}$ and the solution γ_{u_-} does not intersect with γ_{u_+} at some υ such that $\upsilon_{a_+} < \upsilon < \upsilon_{a_-}$, then we can decrease arbitrarily ε as long as it is positive and since $\upsilon_{a_-} = \upsilon_{c_+} + \varepsilon$, then there must exists $\upsilon_{a_+} < \upsilon_x < \upsilon_{a_-}$ such that

$$\gamma_{u_+}(\upsilon_x, c_1(\upsilon_{a_+})) = \gamma_{u_-}(\upsilon_x, c_2(\upsilon_{a_-})).$$

Note now that since γ_{u_-} intersects with c_1 at υ_{b_-}, and γ_{u_+} always increases but remains below c_1 as υ increases, then there must exists $\upsilon_{a_-} < \upsilon_{\max} < \upsilon_{b_-}$ such that

$$\gamma_{u_+}(\upsilon_{\max}, c_1(\upsilon_{a_+})) = \gamma_{u_-}(\upsilon_{\max}, c_2(\upsilon_{a_-})).$$

Finally, by converse arguments, since γ_{u_+} intersects with c_2 at υ_{b_+}, and γ_{u_-} always increases but remains below c_2 as υ decreases, then there must exists $\upsilon_{b_+} < \upsilon_{\min} < \upsilon_{a_+}$ such that

$$\gamma_{u_+}(\upsilon_{\min}, c_1(\upsilon_{a_+})) = \gamma_{u_-}(\upsilon_{\min}, c_2(\upsilon_{a_-})).$$

□

It should be immediately noted from Proposition 3.7 on the accommodation property and from Proposition 4.3 on the existence of an invariant butterfly loop that applying a simple periodic input $u_p \in AC(\mathbb{R}_+, \mathbb{R})$ with only one maximum and one minimum in its periodic interval whose values are $\upsilon_{\min}$ and $\upsilon_{\max}$, then the input-output phase plot will converge to the butterfly hysteresis loop for every initial value of the output $\gamma_0 \in \mathbb{R}$.

A. Example of a Duhem butterfly operator

As an illustrative example, we introduce now a Duhem butterfly operator, which we build constructively by: i). defining arbitrary curves $c_1(\upsilon,\gamma)$ and $c_2(\upsilon,\gamma)$ satisfying conditions of Lemma 4.1; and ii). selecting the functions f_1 and f_2 such that these curves correspond to the zero level set (i.e. $f_1(\upsilon, c_1(\upsilon)) = f_2(\upsilon, c_2(\upsilon)) = 0$) and satisfy the hypotheses in Lemma 4.2 and Proposition 4.3. In general, any functions f_1 and f_2 satisfying hypotheses in Lemmas 4.2, 4.1 and Proposition 4.3, which can be constructed using particular kernel functions or identified using existing models in literature, will produce Duhem butterfly operators.

Let us firstly define the curves c_1 and c_2 by

$$c_1(\upsilon,\gamma) := \quad a_1 + a_2\upsilon + a_3\upsilon^3, \tag{35}$$
$$c_2(\upsilon,\gamma) := -b_1 - b_2\upsilon - b_3\upsilon^3. \tag{36}$$

In order to assign these curves as the zero level sets we can define f_1 and f_2 as the signed vertical distance between the curve $c_1(\upsilon,\gamma)$ and the point (υ,γ), and respectively, between $c_1(\upsilon,\gamma)$ and the point (υ,γ). Here, we need to take care that the convergence conditions (18) and (19) are satisfied. Accordingly, we can define f_1 and f_2 by

$$\begin{aligned} f_1(\upsilon,\gamma) :=& \quad (c_1(\upsilon) - \gamma) \\ =& \quad \left(a_1 + a_2\upsilon + a_3\upsilon^3 - \gamma\right), \end{aligned} \tag{37}$$
$$\begin{aligned} f_2(\upsilon,\gamma) :=& -(c_2(\upsilon) - \gamma) \\ =& \quad \left(b_1 + b_2\upsilon + b_3\upsilon^3 + \gamma\right). \end{aligned} \tag{38}$$

Substituting the functions defined above into (18) and (19) we obtain that

$$-(\gamma_1 - \gamma_2)^2 < 0 \quad \text{and} \quad (\gamma_1 - \gamma_2)^2 > 0,$$

which are trivially satisfied.

In Fig. 8a, we present the simulation results of a Duhem butterfly operator (3) defined with (37) and (38) when a periodic input, whose maximum and minimum are $u_{\max} = 5$ and $u_{\max} = -5$, is applied. As remarked before, our main results in Lemma 4.1, Lemma 4.2 and Proposition 4.3 hold also for the case when the signs are reversed. Correspondingly, in this subsection, we present an example of a Duhem operator that satisfies all the opposite conditions to Lemmas 4.1-4.2 and to Proposition 4.3. We modify slightly the previous example in Subsection IV-A by defining f_1 and f_2 as follows.

$$\begin{aligned} f_1(\upsilon,\gamma) :=& \quad (-c_1(\upsilon) - \gamma) \\ =& \quad \left(-a_1 - a_2\upsilon - a_3\upsilon^3 - \gamma\right), \end{aligned} \tag{39}$$
$$\begin{aligned} f_2(\upsilon,\gamma) :=& -(-c_2(\upsilon) - \gamma) \\ =& \quad \left(-b_1 - b_2\upsilon - b_3\upsilon^3 + \gamma\right). \end{aligned} \tag{40}$$

By vis-á-vis arguments to the ones of Proposition 4.3, a Duhem operator with the above f_1 and f_2 can also produce a hysteresis loops with self-intersections. This will result in the reversion of the loop orientation. Fig. 8b shows a simulation result of a Duhem butterfly operator (3) defined by (39) and (40).

B. Modeling of doped PZT material by Duhem butterfly operator

In this subsection, we present an example of a Duhem butterly operator fitted to experimental data of the sample of piezoelectric material whose relation between electric-field and strain exhibited an asymmetric butterfly hysteresis loop. The sample was made out of doped Lead Zirconate Tinate (PZT), which has been developed for the design of hysteretic deformable mirror [28]. The strain measurements were taken by laser interferometer. The applied input signals were triangular periodic signals of 1400V of amplitude with frequency of 1Hz. For numerical fitting purpose, we use the

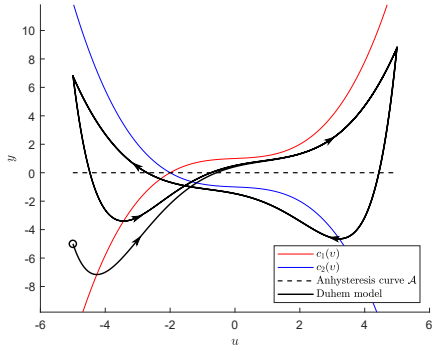

(a) With gradient functions f_1 and f_2 given by (37) and (38).

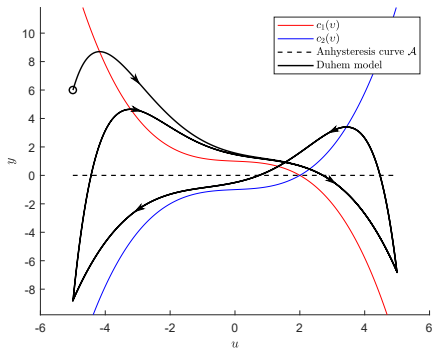

(b) With gradient functions f_1 and f_2 given by (39) and (40).

Figure 8: Butterfly hysteresis loops obtained from a Duhem model whose gradient functions f_1 and f_2 are given by a cubic polynomial under the application of a periodic input whose minimum and maximum are $\upsilon_{\min} = -5$ and $\upsilon_{\max} = 5$. The initial point $(u(0), y(0)) = (\upsilon_{\min}, y_0)$ is marked by a circle.

same kernel vector functions as the ones in Example IV-A using the signed distance between the point (υ, γ) to the two curves $c_1(\upsilon, \gamma)$ and $c_2(\upsilon, \gamma)$, as follows

$$c_1(\upsilon,\gamma) := \sum_{n=0}^{5} a_n \upsilon^n, \qquad c_2(\upsilon,\gamma) := -\sum_{n=0}^{5} b_n \upsilon^n.$$

Therefore, the functions f_1 and f_2 are given by

$$f_1(\upsilon,\gamma) := -\gamma + \sum_{n=0}^{5} a_n \upsilon^n, \quad f_2(\upsilon,\gamma) := \gamma + \sum_{n=0}^{5} b_n \upsilon^n. \quad (41)$$

The identified numerical parameters were $a_0 = -5.1171$, $a_1 = -1.1072$, $a_2 = 0.0608$, $a_3 = 0.0321$, $a_4 = 0.0009$, $a_5 - 0.0001$, $b_0 = 0.2223$, $b_1 = 1.6194$, $b_2 = -0.0806$, $b_3 = -0.0068$, $b_4 = 0.0016$, and, $b_5 = -0.0001$. These fitted parameters were obtained by minimizing the least square error given by the difference between the model output and experimental the data. Fig. 9 shows the input-output phase plot with the experimental data, the simulation results, the level curves $c_1(\upsilon, \gamma)$ and $c_2(\upsilon, \gamma)$, which are constructed based on f_1 and f_2, respectively, and the corresponding anhysteresis curve.

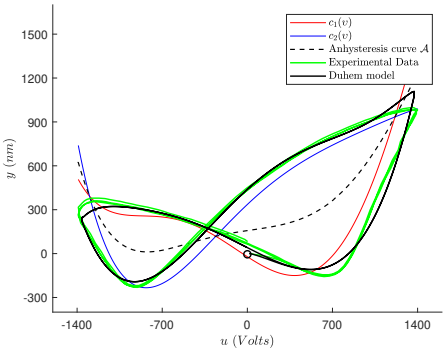

Figure 9: Duhem model whose gradient functions f_1 and f_2 are given by (41) with the parameters fitted to experimental data obtained from a sample of piezoelectric material exhibiting asymmetric butterfly hysteresis behavior. The initial point $(u(0), y(0))$ is marked by a circle.

C. A counter-example of Duhem operator with multi-loop behavior

In this final subsection, we present an example of a Duhem operator that can exhibit multi-loop hysteresis behavior. This is analogous behavior presented in [29] when the Preisach operator weighting function is allowed to have more than two regions of positive and negative values over its domain. In the case of the Duhem operator, its vector functions f_1 and f_2 are no longer restricted to the hypotheses in Lemmas 4.1-4.2 and Proposition 4.3 while they still satisfy the hypotheses in Proposition 3.7.

When the Duhem operator in this example is subjected to a periodic input signal, the input-output phase plot converges to a periodic orbit as expected and additionally the orbit can exhibit multi-loop hysteresis behavior. For constructing this example, we define the zero level set curves c_1 and c_2 by

$$c_1(\upsilon,\gamma) := \ 10\ \sin\left(6\pi\ \upsilon\ +\ \frac{\pi}{8}\right), \quad (42)$$

$$c_2(\upsilon,\gamma) := -\ 8\ \sin\left(6\pi\ \upsilon\ -\ \frac{\pi}{8}\right), \quad (43)$$

and as presented in Subsection IV-A, the functions f_1 and f_2 are defined as the signed vertical distance between these curves (i.e., $c_1(\upsilon, \gamma)$ and $c_2(\upsilon, \gamma)$) and the point (υ, γ), respectively. Explicitly, they are given by

$$\begin{aligned} f_1(\upsilon,\gamma) &:= (c_1(\upsilon) - \gamma) \\ &= 10\ \sin\left(6\pi\ \upsilon\ +\ \frac{\pi}{8}\right) - \gamma, \end{aligned} \quad (44)$$

$$\begin{aligned} f_2(\upsilon,\gamma) &:= -(c_2(\upsilon) - \gamma) \\ &= \ 8\ \sin\left(6\pi\ \upsilon\ -\ \frac{\pi}{8}\right) - \gamma. \end{aligned} \quad (45)$$

The simulation results of such Duhem operator (3) with f_1 as in (44) and f_2 as in (45) are shown in Fig. 10 where multi-loop hysteresis behavior is exhibited.

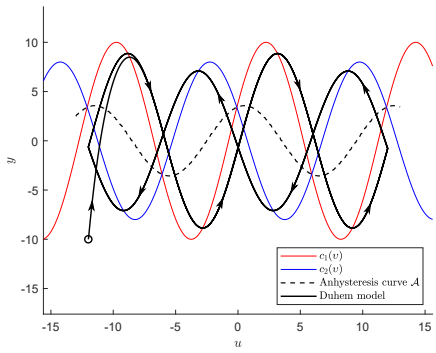

Figure 10: Multi-loop hysteresis loop obtained from a model Duhem model whose gradient functions f_1 and f_2 are given by (37) and (38), respectively, when a periodic input whose minimum and maximum are $\upsilon_{\min} = -12$ and $\upsilon_{\max} = 12$. The initial point $(u(0), y(0)) = (\upsilon_{\min}, y_0)$ is marked by a circle.

V. CONCLUSIONS

In this paper we have studied and presented sufficient conditions for a class of Duhem hysteresis operators that admit butterfly loops. Firstly, we studied general conditions on the functions f_1 and f_2 so that the Duhem operator has the accommodation property. In particular, we do not impose positive definiteness or an explicit form on these functions. Based on the sufficient conditions for the accommodation property, we presented sufficient conditions on f_1 and f_2 such that the corresponding Duhem hysteresis operator is capable of exhibiting butterfly hysteresis loops. Numerical simulations show also the possibility of having multi-loop behavior when these conditions are not satisfied. The work presented in this paper can be the basis for the development of systems identification methods to model butterfly or multi-loop hysteresis phenomena in many electro-mechanical applications based on the use of integro-differential Duhem models.

REFERENCES

[1] J. A. Ewing and H. C. F. Jenkin, "VII. On the production of transient electric currents in iron and steel conductors by twisting them when magnetised or by magnetising them when twisted," *Proceedings of the Royal Society of London*, vol. 33, no. 216-219, pp. 21–23, Jan. 1882.

[2] D. Angeli, J. E. Ferrell, and E. D. Sontag, "Detection of multistability, bifurcations, and hysteresis in a large class of biological positive-feedback systems," *Proceedings of the National Academy of Sciences*, vol. 101, no. 7, pp. 1822–1827, Feb. 2004.

[3] H. R. Noori, *Hysteresis Phenomena in Biology*, ser. SpringerBriefs in Mathematical Methods. Berlin Heidelberg: Springer-Verlag, 2014.

[4] M. Brokate and J. Sprekels, *Hysteresis and Phase Transitions*, ser. Applied Mathematical Sciences. New York, NY: Springer-Verlag New York, 1996, vol. 121.

[5] S. Choudhury and S. Banerjee, "Hysteresis in the sky," *Astroparticle Physics*, vol. 80, pp. 34–89, 2016.

[6] D. Bakas and Y. Makhlouf, "Can the insider-outsider theory explain unemployment hysteresis in OECD countries?" *Oxford Economic Papers*, vol. 72, no. 1, pp. 149–163, Jan. 2020.

[7] S. Poltoratski and F. Tong, "Hysteresis in the Dynamic Perception of Scenes and Objects," *Journal of experimental psychology. General*, vol. 143, Aug. 2014.

[8] F. Ikhouane, "A Survey of the Hysteretic Duhem Model," *Archives of Computational Methods in Engineering*, vol. 25, no. 4, pp. 965–1002, nov 2018.

[9] J. W. Macki, P. Nistri, and P. Zecca, "Mathematical models for hysteresis," *SIAM review*, vol. 35, no. 1, pp. 94–123, 1993.

[10] I. D. Mayergoyz, "Mathematical models of hysteresis," *IEEE Transactions on Magnetics*, vol. 22, no. 5, pp. 603–608, 1986.

[11] A. Visintin, *Differential Models of Hysteresis*, ser. Applied Mathematical Sciences. Berlin, Heidelberg: Springer-Verlag Berlin Heidelberg, 1994, vol. 111.

[12] M. Naser and F. Ikhouane, "Consistency of the Duhem model with hysteresis," *Mathematical Problems in Engineering*, vol. 1, no. 586130, pp. 1–16, 2013.

[13] B. Jayawardhana and V. Andrieu, "Sufficient conditions for dissipativity on Duhem hysteresis model," in *Proceedings of the 48h IEEE Conference on Decision and Control (CDC) held jointly with 2009 28th Chinese Control Conference*, Dec. 2009, pp. 4378–4383, iSSN: 0191-2216.

[14] B. Jayawardhana, R. Ouyang, and V. Andrieu, "Dissipativity of general Duhem hysteresis models," in *2011 50th IEEE Conference on Decision and Control and European Control Conference*, Dec. 2011, pp. 3234–3239, iSSN: 0743-1546.

[15] B. Jayawardhana, R. Ouyang and V. Andrieu, "Stability of systems with the Duhem hysteresis operator: The dissipativity approach," *Automatica*, vol. 48, no. 10, pp. 2657–2662, Oct. 2012.

[16] A. Pavlov, N. van de Wouw, and H. Nijmeijer, "Convergent systems: Analysis and synthesis," in *Control and Observer Design for Nonlinear Finite and Infinite Dimensional systems, LNCIS 322*, T. Meurer, K. Graichen, and E. Gilles, Eds. Berlin, Heidelberg: Springer, 2005, pp. 131–146.

[17] F. Ikhouane, "Characterization of hysteresis processes," *Math. Contr. Sign. Syst.*, vol. 25, no. 3, pp. 291–310, 2013.

[18] P. Van Bree, C. Van Lierop, and P. Van Den Bosch, "Control-oriented hysteresis models for magnetic electron lenses," *IEEE Transactions on Magnetics*, vol. 45, no. 11, pp. 5235–5238, 2009.

[19] J. Oh and D. S. Bernstein, "Semilinear duhem model for rate-independent and rate-dependent hysteresis," *IEEE Transactions on Automatic Control*, vol. 50, no. 5, pp. 631–645, 2005.

[20] F. Ikhouane, "On Babuška's model for asymmetric hysteresis," *Communications in Nonlinear Science and Numerical Simulation*, vol. 95, p. 105650, Apr. 2021.

[21] G.-Y. Gu, L.-M. Zhu, C.-Y. Su, H. Ding, and S. Fatikow, "Modeling and control of piezo-actuated nanopositioning stages: A survey," *IEEE Transactions on Automation Science and Engineering*, vol. 13, no. 1, pp. 313–332, 2016.

[22] L. Dupré, M. De Wulf, D. Makaveev, V. Permiakov, and J. Melkebeek, "Preisach modeling of magnetization and magnetostriction processes in laminated sife alloys," *Journal of applied physics*, vol. 93, no. 10, pp. 6629–6631, 2003.

[23] B. Drinčić, X. Tan, and D. S. Bernstein, "Why are some hysteresis loops shaped like a butterfly?" *Automatica*, vol. 47, no. 12, pp. 2658–2664, 2011.

[24] M. A. Vasquez Beltran, B. Jayawardhana, and R. Peletier, "On the characterization of butterfly and multi-loop hysteresis behavior," *IEEE Transactions on Automatic Control*, pp. 1–1, 2021.

[25] M. A. Vasquez-Beltran, B. Jayawardhana, and R. Peletier, "Asymptotic Stability Analysis of Lur'e Systems with Butterfly Hysteresis Nonlinearities," *IEEE Control Systems Letters*, vol. 4, no. 2, pp. 349–354, 2020.

[26] B. Jayawardhana, M. A. Beltran, W. J. Van De Beek, C. De Jonge, M. Acuautla, S. Damerio, R. Peletier, B. Noheda, and R. Huisman, "Modeling and Analysis of Butterfly Loops via Preisach Operators and its Application in a Piezoelectric Material," in *Proceedings of the IEEE Conference on Decision and Control*, vol. 2018-Decem. Institute of Electrical and Electronics Engineers Inc., jan 2019, pp. 6894–6899.

[27] A. E. M. Schmerbauch, M. A. Vasquez-Beltran, A. I. Vakis, R. Huisman, and B. Jayawardhana, "Influence functions for a novel hysteretic deformable mirror with a high density 2D array of actuators," *arXiv preprint, arXiv:2005.07418*, 2020.

[28] R. Huisman, M. Bruijn, S. Damerio, M. Eggens, S. N. R. Kazmi, A. E. M. Schmerbauch, H. Smit, M. A. Vasquez-Beltran, E. van der Veer, M. Acuautla, B. Jayawardhana, and B. Noheda, "High pixel number deformable mirror concept utilizing piezoelectric hysteresis for stable shape configurations," 2020.

[29] M. A. Vasquez-Beltran, B. Jayawardhana, and R. Peletier, "Recursive Algorithm for the Control of Output Remnant of Preisach Hysteresis

Operator," *IEEE Control Systems Letters*, vol. 5, no. 3, pp. 1061–1066, Jul. 2021.
[30] D. Torres, J. Zhang, S. Dooley, X. Tan, and N. Sepúlveda, "Hysteresis-based mechanical state programming of mems mirrors," *Journal of Microelectromechanical Systems*, vol. 27, no. 2, pp. 344–354, 2018.
[31] P. Zhang, A. Das, E. Barts, M. Azhar, L. Si, K. Held, M. Mostovoy, and T. Banerjee, "Robust skyrmion-bubble textures in SrRuO3 thin films stabilized by magnetic anisotropy," *Physical Review Research*, vol. 2, no. 3, Jul. 2020.
[32] M. Ismail, F. Ikhouane, and J. Rodellar, "The hysteresis Bouc-Wen model, a survey," *Archives of Computational Methods in Engineering*, vol. 16, no. 2, pp. 161–188, jan 2009.
[33] R. Bouc, "Forced vibration of mechanical systems with hysteresis," in *Proceedings of 4th Conference Nonlinear Oscillation*, 1967.
[34] Y.-K. Wen, "Method for Random Vibration of Hysteretic Systems," *Journal of the Engineering Mechanics Division*, vol. 102, no. 2, pp. 249–263, 1976.
[35] F. Blanchini, "Set invariance in control," *Autom.*, vol. 35, no. 11, pp. 1747–1767, 1999.

Marco Augusto Vasquez-Beltran received the B.Sc. degree in electronics engineering from the Instituto Tecnologico de Orizaba, Orizaba, Mexico, in 2013, the M.Sc. degree in electrical engineering from the Centro de Investigación y de Estudios Avanzados (CINVESTAV), Mexico, Mexico, in 2015, and the Ph.D. degree from University of Groningen, the Netherlands, in 2022. His research interests include cyber-physical systems, dynamical systems, and artificial intelligence.

Bayu Jayawardhana (SM'13) received the B.Sc. degree in electrical and electronics engineering from the Institut Teknologi Bandung, Bandung, Indonesia, in 2000, the M.Eng. degree in electrical and electronics engineering from the Nanyang Technological University, Singapore, in 2003, and the Ph.D. degree in electrical and electronics engineering from Imperial College London, London, U.K., in 2006. He is currently professor of Mechatronics and Control of Nonlinear Systems in the Faculty of Science and Engineering, University of Groningen, Groningen, The Netherlands. He was with Bath University, Bath, U.K., and with Manchester Interdisciplinary Biocentre, University of Manchester, Manchester, U.K. His research interests include the analysis of nonlinear systems, systems with hysteresis, mechatronics, systems and synthetic biology. Prof. Jayawardhana is a Subject Editor of the International Journal of Robust and Nonlinear Control, an Associate Editor of the European Journal of Control and a member of the Conference Editorial Board of the IEEE Control Systems Society.

Reynier Peletier (M.Sc. University of Leiden. Ph.D. University of Groningen) has been a postdoc at the Harvard-Smithsonian Center for Astrophysics, a postdoctoral fellow at the European Southern Observatory, and a postdoc in Groningen. In 1997 he obtained a PPARC Advanced Fellowship at the University of Durham, two years later he was appointed as lecturer at the University of Durham, and in 2003 he moved back to Groningen. He is currently a Full Professor at the Kapteyn Astronomical Institute at the University of Groningen. He is interested in the evolution of galaxies, their dynamics and stellar populations, but also in instrumentation for large astronomical telescopes. He has edited several books and written more than 200 papers in refereed journals. At present, he is leading an EU International Training Network, named SUNDIAL, integrating computer scientists and astronomers to develop novel data analysis techniques for use in astronomy.